Absolute quantification reveals microbial and component dynamics in spontaneously fermented *Sojae Semen Praeparatum*

Chaojie Yang[1], Guangzong He[1], Junhao Li[2], Mengfei Gao[1], Kexin Fang[1], Chuying Huang[1], Shanshan Mei[1], Dan Jiang[1,*], Yaojun Yang[1,*]

[1]School of Chinese Materia Medica, Beijing University of Chinese Medicine, Beijing, China; [2]The First Department of Orthopaedics, Dongzhimen Hospital, Beijing University of Chinese Medicine, Beijing, China

***Corresponding Author:** Yaojun Yang, Department of Traditional Chinese Medicine Resources and Identification, School of Chinese Materia Medica, Beijing University of Chinese Medicine, Sunshine South Street, Fangshan District, Beijing 102488, China. Email: yangyaoj002@sina.com; Dan Jiang, School of Chinese Materia Medica, Beijing University of Chinese Medicine, Beijing 102488, China. Email: jiangdan1027@163.com

Academic Editor: Sedat Sayar**,** PhD, Department of Food Engineering, Mersin University, Mersin, Turkey

Received: 29 April 2025; Accepted: 18 November 2025; Published: 10 February 2026

ORIGINAL ARTICLE

Abstract

Sojae Semen Praeparatum (*SSP*) is a traditional food and medicine. This study aimed to elucidate microbial succession during fermentation and its correlations with key metabolites. An absolute quantitative sequencing (AQS) approach was employed, which quantifies microbial copy numbers and accounts for changes in total microbial load across fermentation stages to accurately capture microbial succession. *SSP* samples from both koji-making and post-fermentation were analyzed using AQS, GC-MS, and physicochemical profiling. Progressive increases were observed in free isoflavones, polyphenols, ammonia nitrogen (AN), total acids, and water-/alcohol-soluble extracts. GC-MS identified 54 volatiles, mainly acids, esters, and amines, showing stage-specific variations. AQS revealed *Bacillus* and *Aspergillus flavus* as dominant during koji-making, while *Pediococcus* and *Enterococcus* predominated in the post-fermentation stage, representing a new insight into *SSP* succession. Significant correlations ($|r| > 0.8$, $p < 0.05$) were observed between dominant taxa and key components (e.g., isoflavones, polyphenols, AN, and 21 volatiles). Interestingly, this study discusses dual roles of dominant taxa in producing both beneficial components (e.g., isoflavones and polyphenols) and potential risk compounds (e.g., biogenic amines and aflatoxins). These findings highlight AQS as a powerful tool for investigating complex microbial dynamics and provide a basis for optimizing *SSP* fermentation and quality management.

Keywords: Absolute Quantitative Sequencing; Fermentation; Microorganisms; Quality; *Sojae Semen Praeparatum*

Introduction

Soybean-based fermented foods have gained global popularity not only for their distinctive flavors but also for their remarkable health-promoting properties (An *et al.*, 2023). Diverse fermentation methodologies developed across different regions have produced a wide range of soybean-derived fermented products, each with unique

ISSN 1757-837X online, DOI 10.15586/qas.v18i1.1604

aromatic profiles, textural characteristics, and functional properties. Examples include Chinese *Douchi* (Zhao *et al.*, 2025), *Sufu* (Liu *et al.*, 2025), and Korean *Ganjang* (Lim *et al.*, 2025). Within China, *Sojae Semen Praeparatum* (*SSP*) represents a special type of *Douchi*. It is uniquely prepared through natural fermentation combined with herbal juices. This traditional Chinese medicinal product has dual functionality, serving both therapeutic purposes and culinary applications (Li *et al.*, 2021). Previous studies have shown that *SSP* contains typical bioactive compounds, such as flavonoids, polyphenols, and organic acids, commonly found in other fermented soybean products (Lin *et al.*, 2021). In addition, *SSP* possesses a complex profile of volatile components (Guo *et al.*, 2024; Wang *et al.*, 2024). These key chemical constituents (isoflavonoids, polyphenols, organic acids, and volatile compounds) and critical physicochemical properties (e.g., pH, total acids (TAs), ammonia nitrogen (AN), and moisture content)) are recognized as fundamental indicators reflecting the fermentation progress and product quality of *Douchi* (Sui *et al.*, 2024; Liu *et al.*, 2020). Collectively, these chemical constituents provide the essential material basis for *SSP*'s therapeutic efficacy in treating fever-related conditions. Therefore, monitoring the dynamic changes of these specific parameters during *SSP* fermentation is crucial to understand the underlying biochemical processes and establish quality control benchmarks.

Microorganisms play a significant role in shaping these compositional changes during *SSP* fermentation. For instance, Xiong *et al.* (2019) have identified nine bacterial strains capable of producing γ-aminobutyric acid in *SSP*, while Zhao *et al.* (2022) demonstrate that co-fermentation with *Rhizopus chinensis* 12 and *Bacillus sp.* DU-106 substantially increases isoflavone content. More recently, Guo *et al.* (2024) and Wang *et al.* (2024) link core bacterial genera to the formation of *SSP* flavor compounds. Conventional microbial sequencing, however, provides only relative quantification, which limits the analysis of microbial dynamics. This limitation is particularly critical because key processes, such as koji-making and washing, can drastically alter total microbial biomass. Relying solely on relative abundance may introduce systematic bias by ignoring absolute differences in microbial load across samples. To address this, we applied absolute quantitative sequencing (AQS) using synthetic spike-in sequences. These spike-ins were added to samples at known concentrations and processed together with sample DNA. Microbial absolute copy numbers were then calculated by calibrating target reads against spike-in reads, enabling direct measurement of microbial load and unbiased comparisons between samples in spite of variations in biomass (Yao *et al.*, 2024).

In spite of the well-established fermentation process of *SSP*, significant regional variations persist in the microbial composition and abundance under natural fermentation conditions. For example, Zhu *et al.* (2015) have identified *Bacillus subtilis* and *Aspergillus* spp. as the dominant microorganisms during the koji-making stage of *SSP* in Jiangxi Province using Biolog technology. In contrast, Liu *et al.* (2021) report *Neurospora crassa* and *Aspergillus* spp. as the dominant fungal taxa at the same stage in Fujian Province based on ITS sequencing. Studies from Chengdu by Guo *et al.* (2024) and Wang *et al.* (2024) further highlight geographical divergence: Nostocaceae and Enterobacteriaceae dominate the koji-making stage, whereas *Leuconostoc* and *Aspergillus* prevail post-fermentation. These findings collectively underscore substantial regional heterogeneity in *SSP* fermentation microbiota, which can directly affect the stability and consistency of the final product. Identifying the core microbial community in *SSP* is therefore essential for developing relatively controlled inoculated fermentation processes. To address the current research gap, which has focused primarily on southern China, this study selected Beijing—a representative city in northern China—as the research site. This approach allows for comparison with previous studies while significantly expanding the documented diversity of *SSP* fermenting microbiota. The results not only enhance our understanding of potential core starter cultures but also provide more options for inoculated fermentation aimed at improving quality control.

In short, given the critical role of microbial succession in shaping the metabolic profile and final quality of fermented foods, this study aims to elucidate key microbial and functional changes and their potential interactions during *SSP* fermentation in Beijing, China. We employed AQS to characterize the temporal succession of bacterial and fungal communities and conducted comprehensive profiling of functional components, such as isoflavones, total polyphenols (TPPs), total saponins (TSs), and volatile compounds. Furthermore, this study seeks to reveal the potential associations between microbial community dynamics and the evolution of *SSP* functional profiles throughout the fermentation process.

Materials and Methods

Fermentation of SSP and sampling

SSP was fermented following the protocol described by Li *et al.* (2014) at the Beijing University of Chinese Medicine, Laboratory C101, Department of TCM Resources and Identification. The process (Figure 1) consisted of the following steps: A mixture of *Mori Folium* (90 g) and *Artemisia Annuae* (100 g) was decocted twice in 2 L of distilled water, each for 1 h. The combined extracts were concentrated to 1 L. Black beans (1 kg) were soaked in

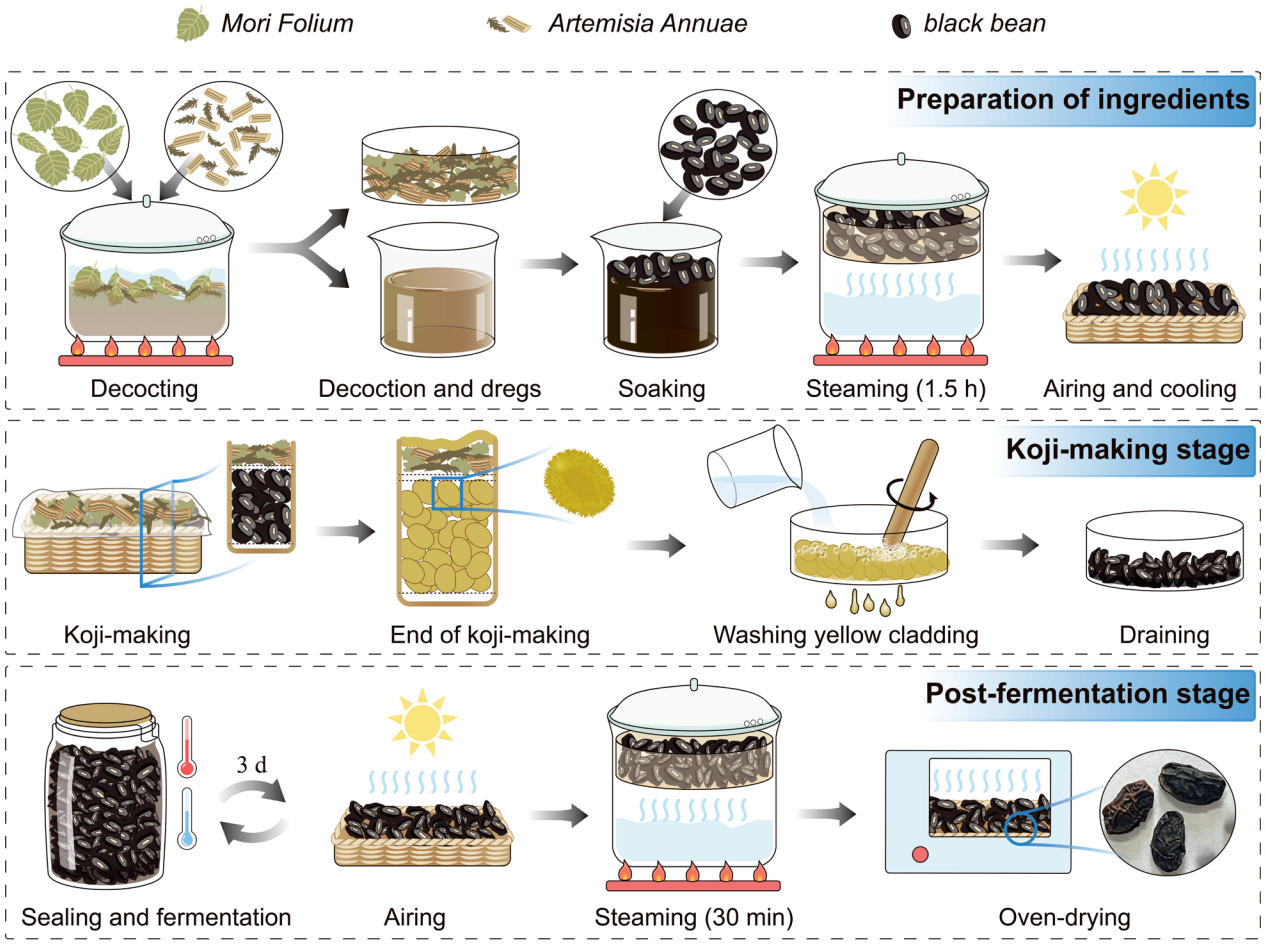

Figure 1. Manufacture process of *Sojae Semen Praeparatum* (*SSP*).

the herbal decoction for 6 h, steam-cooked for 1.5 h, and cooled to room temperature. The beans were then transferred to rattan trays, covered with three layers of sterile cotton gauze and residue herbs, and incubated during the koji-making stage at 30 ± 2°C and 75% relative humidity for 6 days, until a yellow mycelium and spore layer, commonly known as yellow cladding, was formed. Following winnowing and washing, the beans were placed in glass jars for post-fermentation at 30 ± 2°C for 18 days. Finally, *SSP* decoction pieces were obtained after steaming for 0.5 h and drying at 60°C.

Triplicate samples (~200 g each, n = 3) of fresh *SSP* were collected at predefined intervals from the central regions to avoid edge effects: every 2 days during the koji-making stage (days 0, 2, 4, 6; designated K0, K2, K4, K6) and every 3 days during the post-fermentation stage (days 0, 3, 6, 9, 12, 15, 18; designated P0, P3, P6, P9, P12, P15, P18). The final steamed product was labeled PS18. Half of the fresh *SSP* samples were flash-frozen in sterile polyethylene bags and stored at −80°C for DNA extraction and subsequent microbial community analysis, while the remaining samples were used for physicochemical characterization.

To ensure process consistency, five consecutive *SSP* batches were produced prior to sampling. Product quality was assessed according to the Chinese Pharmacopoeia (Ch. P.) 2020 (Commission, 2020) through evaluations of sensory characteristics, purity test, and quantification of bioactive compounds (genistein and daidzein).

Determination of physiochemical properties

The content of TAs was determined by acid-base titration using sodium hydroxide (Liang *et al.*, 2019). AN content was measured using the formaldehyde titration method (Zhao *et al.*, 2019). Water-soluble extracts (WSE), alcohol-soluble extracts (ASE), and moisture content were determined following the Chinese Pharmacopoeia (Ch. P.) 2020 (Commission, 2020). pH values were recorded using a pH meter (FiveEasy Plus, Mettler Toledo Instruments Co., Ltd., Shanghai, China) according to Kim *et al.* (2018). All assays were performed in triplicates (n = 3).

The content of TPPs in *SSP* was determined using a modified Folin–Ciocalteu method (Gao *et al.*, 2000).

Briefly, 1 g of *SSP* powder was ultrasonically extracted with 20 mL of 80% (v/v) methanol. Following centrifugation, the extraction was repeated, and the combined supernatants were then vacuum-dried at 40°C. The residue was reconstituted in 25 mL of 80% (v/v) methanol and centrifuged, and the resulting supernatant was designated as the test solution. For analysis, 0.1 mL of the test solution was mixed with 2.9 mL of water and 0.5 mL of 1 mol/L Folin–Ciocalteu reagent. After standing for 1 min, 0.5 mL of 15% (w/w) sodium carbonate solution was added, and the mixture was incubated in the dark at 25°C for 3 h. The mixture was subsequently diluted to 10 mL with water, and absorbance was measured at 760 nm. A standard curve was prepared using gallic acid solutions ranging from 10 to 50 mg/mL. Each *SSP* sample was analyzed in triplicate (n = 3).

Total polysaccharides (TPSs) were extracted and quantified using a modified phenol-sulfuric acid method (Liu et al., 2022). Briefly, 2 g of *SSP* powder was defatted by soaking in 10 mL of petroleum ether (b.p. 30 ~ 60°C) for 30 min, and the supernatant was discarded; this process was repeated thrice. After complete solvent evaporation, the powder was reflux-extracted twice in 100 mL of distilled water for 1 h each. The combined extracts were filtered, concentrated under vacuum at 60°C, and redissolved in distilled water to a final volume of 25 mL. A 5 mL aliquot was precipitated by adding four volumes of ethanol. After centrifugation, the precipitate was dissolved in 10 mL of distilled water. Deproteinization was performed by mixing the solution with 1/4 volume of Sevag reagent (chloroform: n-butanol = 4: 1, v/v), followed by centrifugation at 5000 × g for 5 min. The supernatant was collected, and the Sevag treatment was repeated thrice. The final polysaccharide extract was stored at 4°C prior to analysis. TPSs' content was determined using the phenol-sulfuric acid method. Briefly, 0.1 mL of polysaccharide extract was diluted to 2 mL with distilled water, mixed with 1 mL of 5% (w/v) phenol, and then rapidly mixed with 5 mL of concentrated sulfuric acid. The mixture was incubated in a boiling water bath for 10 min, cooled immediately in ice water, and absorbance was measured at 485 nm. A standard curve was prepared using glucose solutions ranging from 10 to 50 mg/mL. Each *SSP* sample was analyzed in triplicate (n = 3).

TSs' content was determined using a modified vanillin-phenol-perchloric acid method (Wang *et al.*, 2014). Briefly, 1 g of *SSP* powder was defatted with petroleum ether as described for polysaccharide extraction. The defatted powder was ultrasonically extracted twice with 20 mL of ethanol, followed by centrifugation. The combined supernatants were concentrated under reduced pressure at 45°C. The concentrate was dissolved in 20 mL of distilled water and partitioned thrice with an equal volume of water-saturated n-butanol in a separatory funnel. The combined n-butanol phases were vacuum-dried at 60°C. The residue was dissolved in 25 mL 80% (v/v) ethanol and stored at 4°C prior to analysis. For quantification, 0.2 mL of the test solution was evaporated to dryness at 60°C. After cooling, the residue was dissolved in 0.2 mL of 5% (w/v) vanillin in glacial acetic acid, and 0.8 mL of perchloric acid was added. The reaction mixture was incubated in a 70°C water bath for 15 min, cooled in and ice bath, and then diluted to 10 mL with ethyl acetate. The solution was kept on ice, and absorbance was measured at 550 nm within 1 h. A standard curve was established using oleanolic acid solutions ranging from 10 to 50 mg/mL. Each *SSP* sample was analyzed in triplicate (n = 3).

UPLC analysis of isoflavones

The six isoflavones (daidzein, daidzin, genistein, genistin, glycitein, and glycitin) in *SSP* were quantified using ultra-performance liquid chromatography (UPLC). Briefly, 1 g of *SSP* powder was ultrasonically extracted with 25 mL of 75% (v/v) methanol at 40°C for 40 min and centrifuged at 6000 × g and 4°C for 15 min. The supernatant was filtered through a 0.22 μm nylon membrane before UPLC analysis. Accurately weighed reference standards (10 mg each) were dissolved in methanol to prepare individual stock solutions (250 μg/mL). Working calibration standards were prepared by combining appropriate aliquots of stock solutions and preforming serial dilutions with methanol. UPLC analysis was performed on an ACQUITY H-Class system (Waters Cor., Milford, MA, USA) equipped with an ACQUITY UPLC BEH C18 column (2.1 mm × 100 mm, 1.7 μm; Waters Corp., Dublin, Ireland). The mobile phase consisted of 0.1% formic acid in acetonitrile (solvent A) and 0.1% formic acid in water (solvent B). Gradient elution was carried out as follows: 0 ~ 5 min, 12 ~ 20% A; 5 ~ 8 min, 20% A; 8 ~ 13 min, 20 ~ 35% A; 13 ~ 15 min, 35% A; 15 ~ 16 min, 35 ~ 50% A; 16 ~ 17 min, 50 ~ 12% A; 17 ~ 18 min, 12% A. The flow rate was 0.35 mL/min, the detection wavelength was 260 nm, the column temperature was 30°C, and the sample temperature was 20°C. The injection volume was 1 μL. Each sample was analyzed in triplicate (n = 3).

GC-MS analysis of volatile compounds

Volatile metabolites were analyzed using gas chromatography-mass spectrometry (GC-MS). One gram of *SSP* powder was spiked with 348.8 μg of methyl undecanoate (internal standard) and extracted with 20 mL ethyl acetate under ultrasonication (250 W, 40 min). The extract was filtered through a 0.22 μm nylon membrane prior to GC-MS analysis. The analysis was performed on a GC-MS system (7890B GC coupled with 5977C MSD, Agilent Technologies Inc., Santa Clara, CA, USA). Separation was achieved on a BP-Inowax-MS capillary column (30 m × 0.25 mm, 0.25 μm; NanoChrom

Table 1. The oven temperature program of GC-MS.

Rate (°C/min)	Value (°C)	Hold time (min)
0	80	2
7	180	10
5	210	10
1	215	20
5	240	20

Technologies Co., Ltd., Suzhou, China) using helium as the carrier gas at a constant flow rate of 1.0 mL/min. The inlet temperature was maintained at 230°C, and the hydrogen, air, and tail blow gas flow rates were set to 30, 300, and 25 mL/min, respectively. Samples were injected at a volume of 1 μL with a split ratio of 50: 1. The oven temperature program followed the conditions listed in Table 1. The mass spectrometer operated with an ion source temperature of 230°C, a transfer line temperature of 240°C, and a scan range of 40 ~ 500 *m/z*. Each *SSP* sample was analyzed in triplicate (n = 3).

Extraction of microbial genome and sequencing

Microorganisms in the *SSP* samples were pre-enriched as described by Xu *et al.* (2020), followed by genomic DNA extraction using the Fast DNA™ SPIN Kit for soil (MP Biomedicals, California, USA). The preparation procedure was as follows. Briefly, 2 g of fresh *SSP* sample was homogenized with 6 mL of sterile washing solution (0.1 mol/L Tris-HCl, pH 8.0, 0.25% Tween 80) by vortexing for 2 min. After centrifugation (200 × g, 4°C, 5 min), the pellets were resuspended and washed once under the same conditions. The combined supernatants were filtered through a single layer of sterile gauze and centrifuged again (10,000 × g, 4°C, 10 min). The resulting pellet was weighed and processed according to the manufacturer's instruction for DNA extraction. All solutions were membrane-filtered (0.22 μm) and stored at 4°C. Biological replicates were processed in quintuplicate (n = 5).

DNA integrity was assessed by 1% agarose gel electrophoresis. DNA concentration and purity were measured using a fluorometer (Qubit 3.0, Thermo Fisher Scientific Inc., Waltham, MA, USA) and a spectrophotometer (NanoDrop 2000, Thermo Fisher Scientific Inc., Waltham, MA, USA). Multiple spike-ins were artificially synthesized, each containing the same conserved regions as natural 16S rRNA genes but with variable regions replaced by random sequences with approximately 40% GC content. A spike-in mixture with known gradient copy numbers was then added to the DNA samples at appropriate ratios. For bacterial sequencing, the V3-V4 hypervariable regions of the 16S rRNA gene and spike-ins were amplified using primers 341F (5'-CCTACGGGNGGCWGCAG-3') and 805R (5'-GACTACHVGGGTATCTAATCC-3'). For fungal sequencing, the ITS1 region and spike-ins were amplified using primers (5'-CTTGG TCATTTAGAGGAAGTAA-3') and (5'-GCTGCGT TCTTCATCGATGC-3'). The resulting PCR products were verified, purified, and quantified, after which sequencing was performed on a NovaSeq 6000 platform (Illumina Inc., San Diego, CA, USA) by Genesky Biotechnologies Inc., Shanghai, China (Jiang *et al.*, 2019).

Statistical analysis

The content (mass fraction) of each physicochemical property was calculated based on the sample mass and analyzed using Origin 2021 software (OriginLab Corp., Northampton, MA, USA). Volatile compounds were identified by comparing mass spectra with those in the NIST 14.0 database. Quantification of volatile components was performed by normalizing chromatographic peak areas to the internal standard (methyl undecanoate) with a known concentration. Statistical analyses were conducted using SPSS 20.0 (IBM Corp., Armonk, NY, USA). Group differences were evaluated using one-way multivariate analysis of variance, with p-values indicating statistical significance. Mean values of the measured indicators were used for fold change (FC) calculations and correlation analyses.

For microbial analysis, QIIME 2 was used to process the raw sequencing data (Bolyen *et al.*, 2019). After trimming adapter and primer sequences using the Cutadapt plugin, the DADA2 plugin was applied to denoise the sequences, identify amplicon sequence variants (ASVs), exclude low-quality reads and potential chimeras, and merge paired-end sequences (Callahan *et al.*, 2016). Taxonomic annotation of the resulting ASVs was performed using the Naive Bayes classifier with reference to the SILVA v.138 database. After identifying the spike-in sequences and quantifying their read counts, a standard curve was generated for each sample by plotting the read counts against the known spike-in copy numbers. This standard curve was then used to calculate the absolute copy number of each ASV in the sample based on its corresponding reads. Because the spike-in sequences were exogenous and did not represent members of the native microbial community, they were removed from subsequent analyses. All ASVs for each species were systematically recorded using Microsoft Excel 2021. Diversity analyses were performed using R software (version 3.5.1), whereas microbial composition analysis, Spearman correlation analysis, and principal component analysis (PCA) were conducted using Origin 2021.

Results

Quality evaluation of five batches of SSP

SSP samples collected at different time points were shown in Figures S1 and S2. Characteristics of the five batches were presented in Figure S3. All samples exhibited similar shape and size, with brownish-black, rugose surfaces featuring a black elongated oval hilum. The texture was soft yet slightly brittle. The cross-section appeared reddish-brown to dark brown with an oily luster. Samples exhibited a strong sauce aroma and a slightly sour-sweet taste. The biuret color reaction for purity testing yielded negative results (Figure S4). Total daidzein and genistein contents across batches were 0.169%, 0.202%, 0.172%, 0.173%, and 0.152%, respectively.

Changes of physicochemical properties

UPLC chromatograms of the six isoflavones were presented in Figure 2. Validation routines of UPLC were provided in Text A1. During fermentation, the contents of isoflavone glycosides decreased (Figure 3A), while those of free isoflavones increased (Figure 3B). TPPs increased from 0.34% (K0) to 1.56% (P18), and then decreased slightly to 1.37% (PS18) after steaming. TSs increased during the koji-making stage, while TPSs remained relatively stable throughout the fermentation process (Figure 3C). TAs, AN, WSE, and ASE showed increasing trends over time (Figure 3D; Figure 3E). The pH values decreased during fermentation, showing an inverse pattern relative to TAs (Figure 3F). Moisture content decreased during the koji-making stage (Figure 3G) and remained at approximately 55% during post-fermentation. PCA showed that PC1 (14.5%) and PC2 (74.5%) together explained 89% of the total variance (Figure 4A). The loading plot (Figure 4B) presented the contributions of genistein, daidzein, WSE, ASE, TAs, AN, and TPPs to PC1.

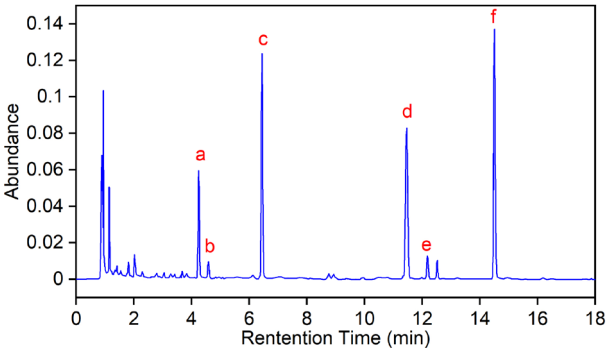

Figure 2. UPLC chromatogram of six isoflavones in *SSP* sample P12 (post-fermentation day 12). Peaks: a, daidzin; b, glycitin; c, genistin; d, daidzein; e, glycitein; and f, genistein.

Changes of volatile components

The total ion chromatogram (TIC) presented in Figure 5 showed the identification and quantification of 54 volatile components, including 13 organic acids, 16 esters, 3 alcohols, 12 amines, 2 aldehydes, 3 ketones, 1 phenol, and 4 other components (Figure S5). The total volatile content increased during fermentation, reaching 17.36 mg/g (P9), followed by a decline during post-fermentation and a further decrease to 9.55 mg/g after steaming (PS18). Except for esters, all volatile categories showed reductions in total content following steaming. Organic acids decreased from 15.26 mg/g to 7.55 mg/g, whereas ester content increased from 0.47 mg/g to 1.05 mg/g (Table S1).

Variations across different stages were presented in the scatter plot (Figure 6). After the koji-making stage (Figure 6A), 37 components were significantly upregulated (FC > 2, $p < 0.01$). Following the post-fermentation stage (Figure 6B), 20 components were significantly upregulated (FC > 2, $p < 0.01$). After steaming (Figure 6C), 5 components increased, while 18 components, including amines and organic acids, significantly decreased (FC > 2, $p < 0.01$). An additional threshold, requiring component concentrations at each stage endpoint to exceed 10 μg/g, was applied to identify key metabolites, which were marked in the bubble plot (Figure 7). After the koji-making stage (Figure 7A), 20 key metabolites were identified, including 9 organic acids, 6 esters, 2 alcohols, 2 amines, and 1 phenazine. The post-fermentation stage (Figure 7B) yielded 11 key metabolites: 3 esters, 3 amines, 2 alcohols, 2 cyclic peptides, and 1 acid. After steaming (Figure 7C), 5 key metabolites were identified, all of which were esters.

Quality control of sequencing data

Gel electrophoresis of microbial genomic DNA showed clear bands (Figure S6), and DNA purity and concentration were suitable for sequencing. Illumina sequencing generated 10,489,297 V3-V4 reads and 8,506,274 ITS reads. The raw data were deposited in the NCBI database (BioProject No. PRJNA1184323). After quality filtering, more than 80% of the initial sequences were retained, showing consistent length distributions and no miscellaneous fragments. The dilution curves (Figure S7) approached a plateau as sequence numbers increased, indicating that the sequencing depth was adequate for community assessment.

The succession of microbial community during SSP fermentation

A comparison of absolute and relative abundances was presented in Figure 8. A total of 86 bacterial

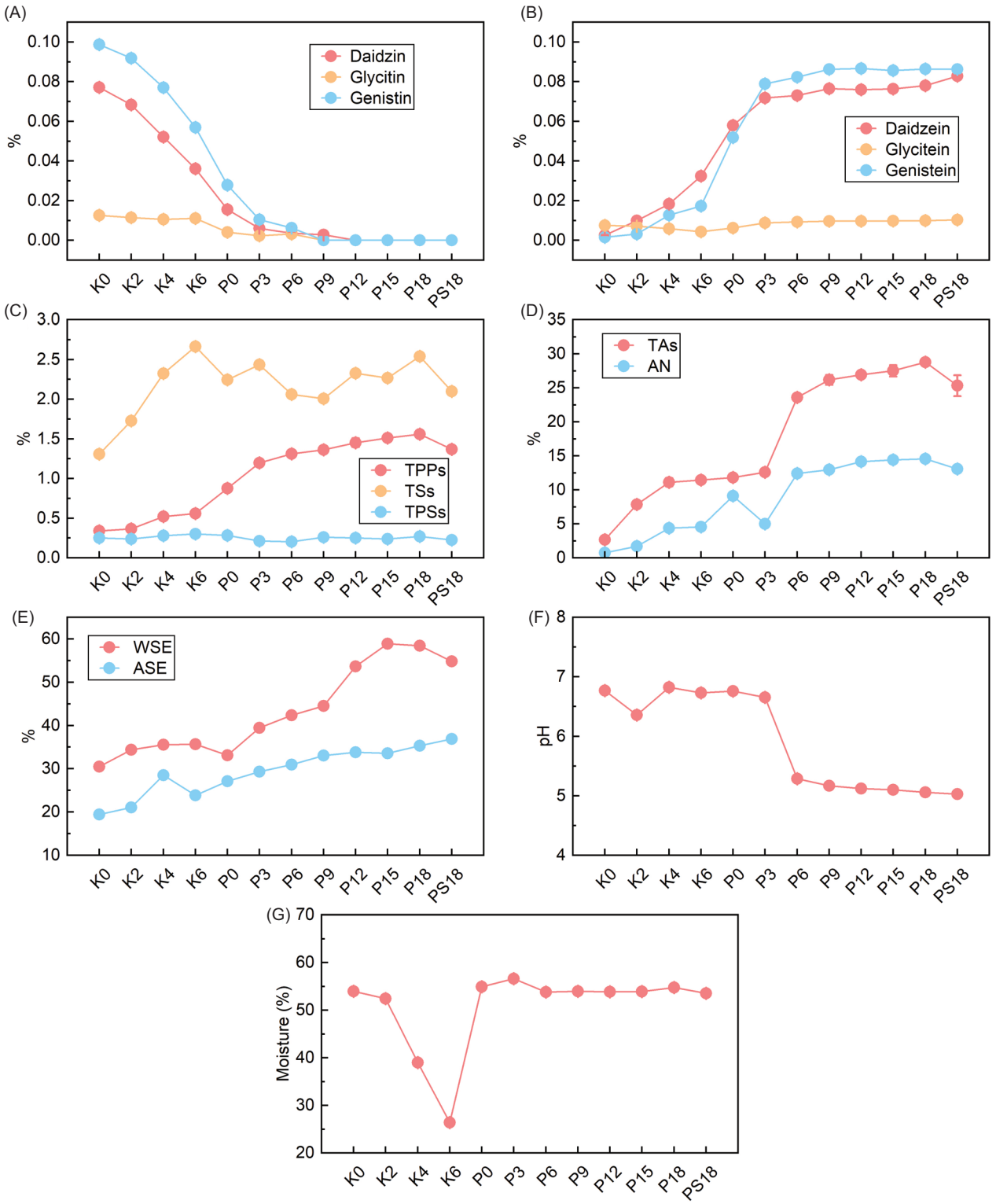

Figure 3. Physicochemical dynamics of *SSP* during fermentation. (A) Three isoflavone glycosides. (B) Three free isoflavones. (C) Total polyphenols (TPPs), total polysaccharides (TPSs), and total saponins (TSs). (D) Total acids (TAs) and ammonia nitrogen (AN). (E) Water-soluble extracts (WSE) and alcohol-soluble extracts (ASE). (F) pH. (G) Moisture content. K0, K2, K4, and K6: samples collected at 0, 2, 4, and 6 days during the koji-making stage; P0, P3, P6, P9, P12, P15, and P18: samples collected at 0, 3, 6, 9, 12, 15, and 18 days during the post-fermentation stage. PS18: steamed product after 18 days of post-fermentation. Data represent mean ± SD, *n* = 3.

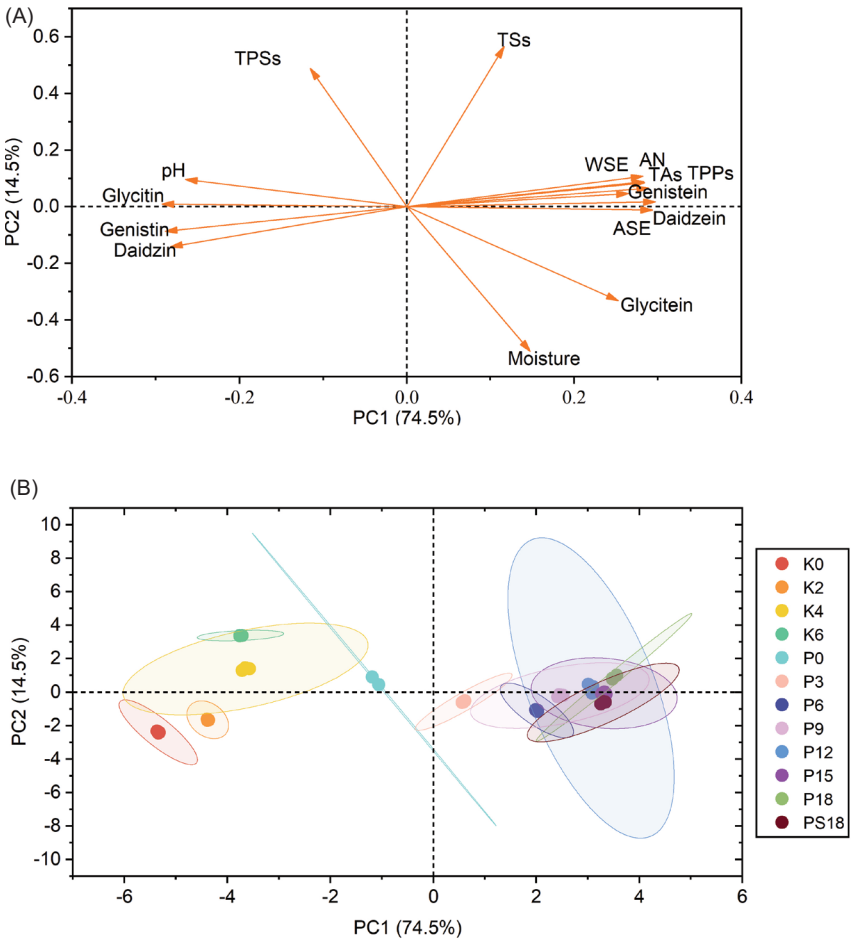

Figure 4. Principal component analysis (PCA) of physicochemical profiles of *SSP* during fermentation. (A) PCA score plot with 95% confidence ellipses. (B) PCA loading plot. K0, K2, K4, and K6: samples collected at 0, 2, 4, and 6 days during the koji-making stage; P0, P3, P6, P9, P12, P15, and P18: samples collected at 0, 3, 6, 9, 12, 15, and 18 days during the post-fermentation stage. PS18: steamed product after 18 days of post-fermentation. *n* = 3 for each sample.

genera from 61 families were identified (Table S2). At the family level, Lactobacillaceae, Enterococcaceae, Bacillaceae, and Enterobacteriaceae accounted for 45.3%, 20.7%, 20.1%, and 13.3%, respectively. During the koji-making stage, *Bacillus* showed a relative abundance of 96.7%, and its absolute abundance increased from 1,331,972 copies (K0) to 3,946,827 copies (K6). Minor populations of *Franconibacter*, *Enterococcus*, *Acinetobacter*, and *Streptophyta* were also detected, each remaining below 4% of *Bacillus*. After removal of the yellow cladding, the abundance of all taxa was reduced. At the onset of post-fermentation, *Enterobacter* (18.6%), *Enterobacteriaceae Unassigned* (23.2%), *Enterococcus* (24.2%), and *Pediococcus* (25.7%) had relative abundances in a similar range. From P12 onwards, *Pediococcus* and *Enterococcus* further increased. Their relative abundances reached 64.4% and 25.7%, respectively. During the same period, *Bacillus* and other genera decreased to relative abundances below 5%.

Fungal succession at the species level was shown in Figure 9. All fungal sequences were annotated to 58 genera from 48 families (Table S2). At the family level, Aspergillaceae accounted for 98.3%, followed by Rhizopodaceae (0.7%), Chaetomiaceae (0.5%), Nectriaceae (0.2%), and Cladosporiaceae (0.1%). During the first 2 days of the koji-making stage, *Aspergillus flavus* reached a relative abundance of 94.9%. Other fungi, including *Aspergillus Unassigned*, *Rhizopus arrhizus*, and *Chaetomium pachypodioides*, had relative abundances below 5%. After the removal of the yellow cladding, the absolute abundance of *A. flavus* was reduced and remained low in subsequent stages.

Correlation of microbial communities and components

Correlation at the koji-making stage

Spearman correlation analysis was performed between all microbial taxa and physicochemical components

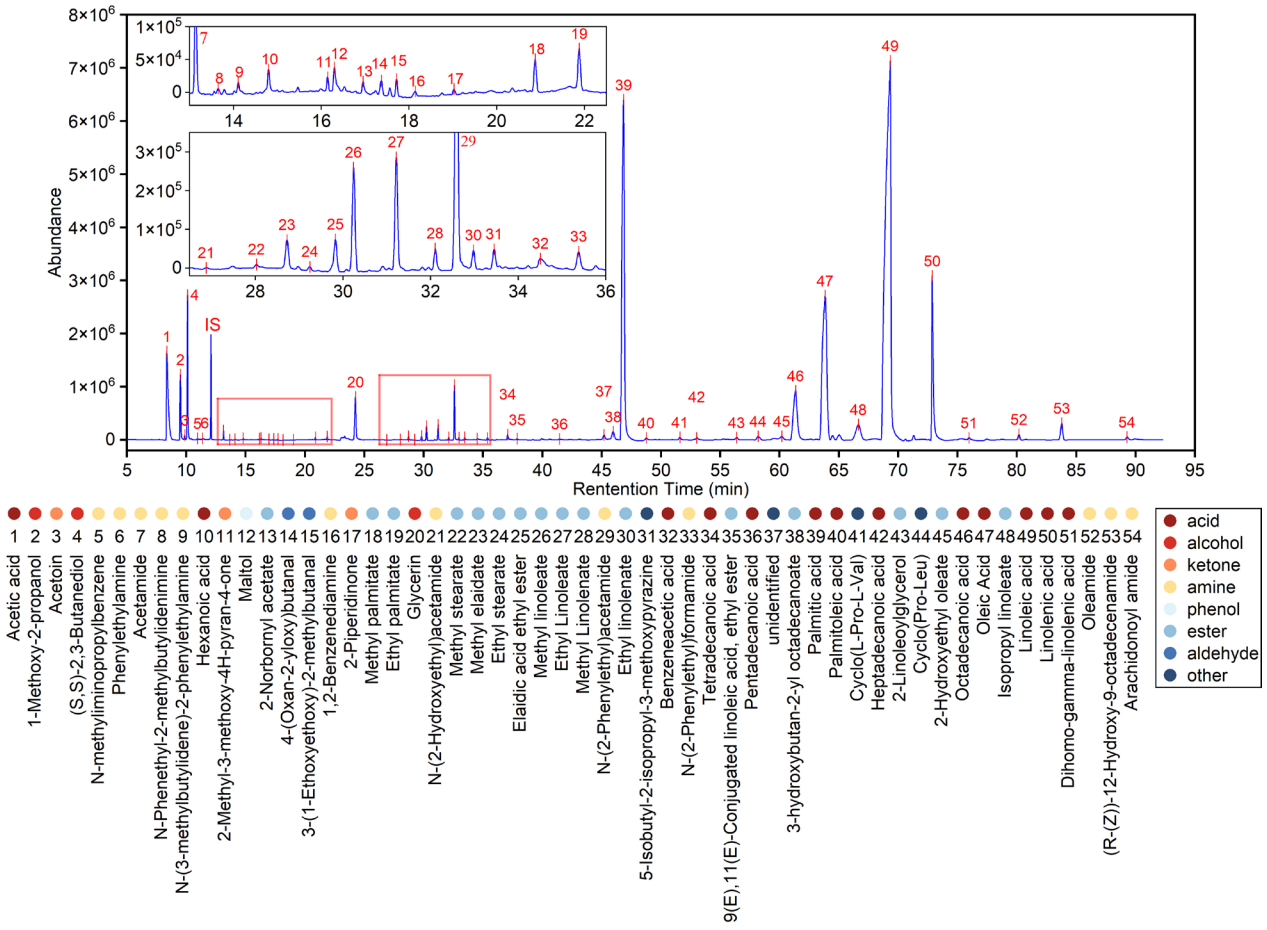

Figure 5. Total ion chromatogram (TIC) of *SSP* sample P12 obtained by GC-MS. IS denotes the inner standard (methyl undecanoate).

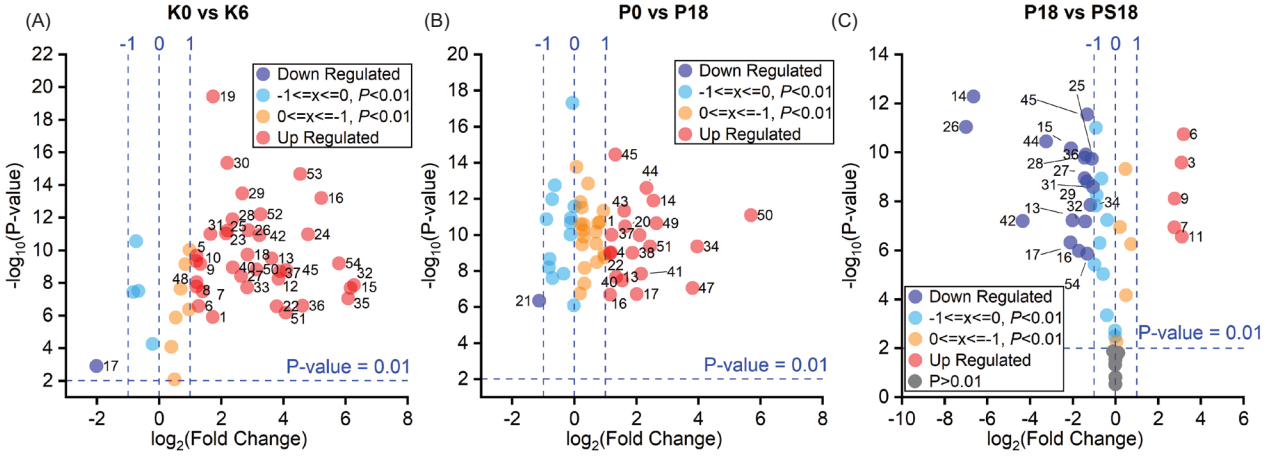

Figure 6. Scatter plots comparing volatile metabolites across *SSP* preparation stages. (A) Koji-making stage. (B) Post-fermentation stage. (C) Steaming stage. Numerical identifiers correspond to peak assignments in Figure 5. K0 and K6: samples collected at 0 and 6 days during koji-making. P0 and P18: samples collected at 0 and 18 days during post-fermentation. PS18: steamed product after 18 days of post-fermentation. Data represent mean ± SD, *n* = 3.

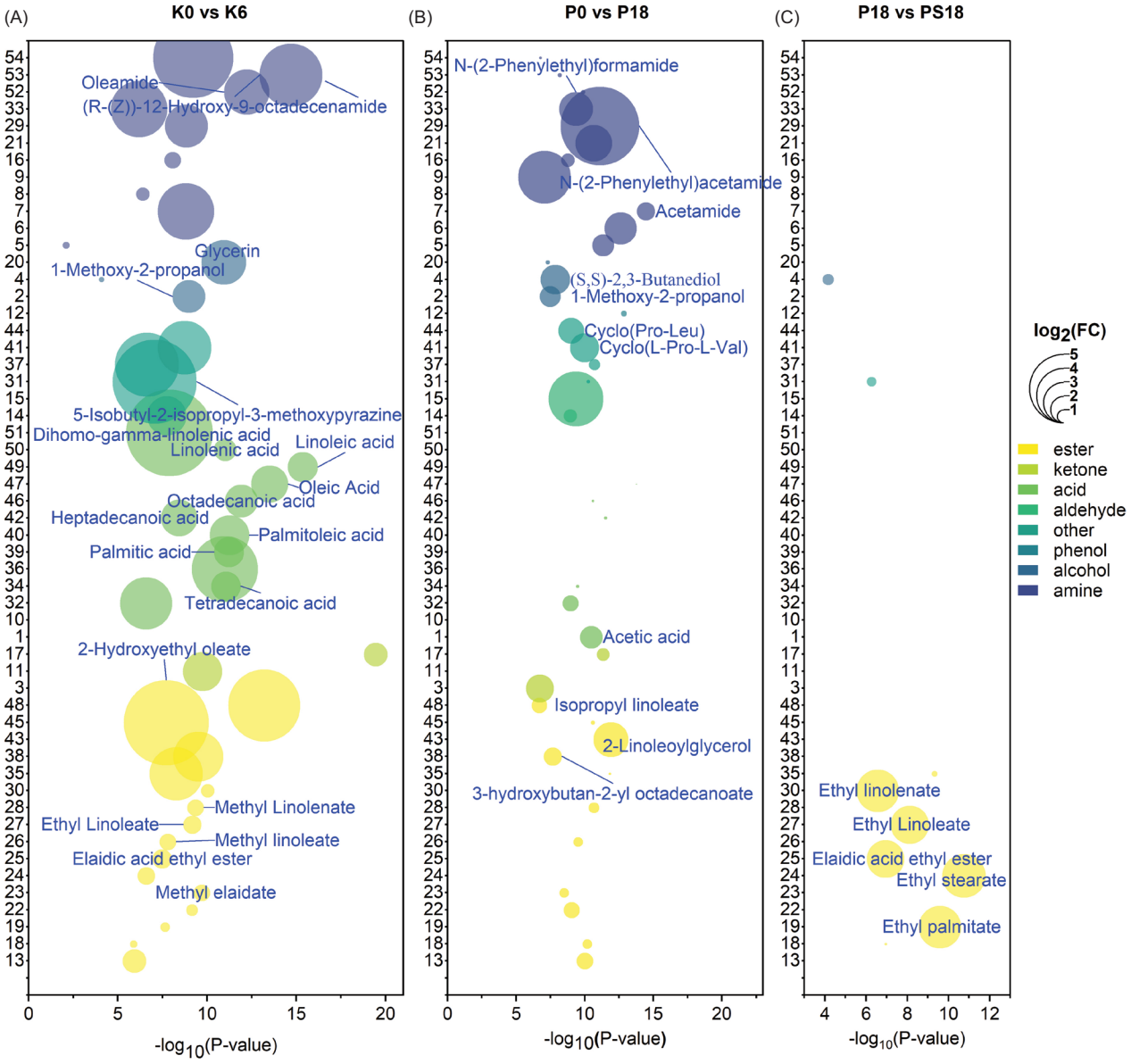

Figure 7. Bubble plots showing changes in volatile metabolites during *SSP* preparation. (A) Koji-making stage. (B) Post-fermentation stage. (C) Steaming stage. Only compounds with content > 10 μg/g, FC > 2, and $p < 0.01$ were labeled. K0 and K6: samples collected at 0 and 6 days during koji-making. P0 and P18: samples collected at 0 and 18 days during post-fermentation. PS18: steamed product after 18 days of post-fermentation. Data represent mean ± SD, $n = 3$.

during the koji-making stage. Twelve bacterial genera were identified with significant associations (Figure 10). *Bacillus*, *Terribacillus*, and *Paenibacillus* showed strong positive correlations ($|r| > 0.8$, $p < 0.05$) with WSE, AN, TAs, free isoflavones, and TPPs. They were also significantly correlated with a wide range of volatile compounds, predominantly esters and acids. *Pediococcus* was positively correlated with TAs. An unclassified Enterobacteriaceae genus showed a unique positive correlation with several esters, including methyl palmitate, methyl elaidate, 2-hydroxyethyl oleate, and isopropyl linoleate. Among fungi, six species exhibited associations with the physicochemical properties measured in this study. These included four *Aspergillus* species (*A. flavus*, *A. Unassigned*, *A. navahoensis*, and *A. pseudodeflectus*). *A. flavus* and *A. Unassigned* displayed correlation profiles similar to *Bacillus*. In contrast, *Chaetomium pachypodioides* and *Fusarium equiseti* displayed different correlation patterns. *C. pachypodioides* was mainly correlated with ethyl esters.

Correlation at the post-fermentation stage

Spearman correlation results between microbes and components during the post-fermentation stage were

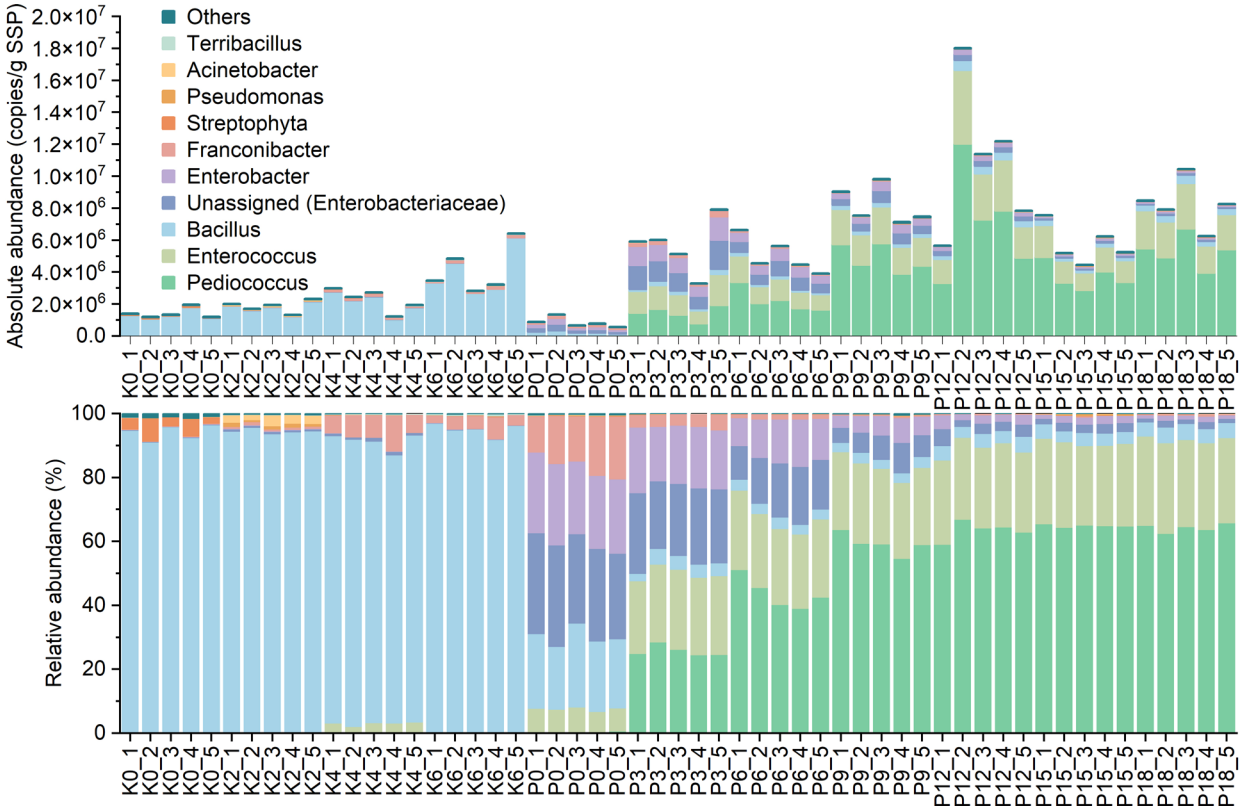

Figure 8. Bacterial community composition at the genus level during *SSP* fermentation. (A) Absolute abundance. (B) Relative abundance. K0, K2, K4, and K6: samples collected at 0, 2, 4, and 6 days during the koji-making stage; P0, P3, P6, P9, P12, P15, and P18: samples collected at 0, 3, 6, 9, 12, 15, and 18 days during the post-fermentation stage. PS18: steamed product after 18 days of post-fermentation. Data represent mean ± SD, *n* = 5.

shown in Figure 11. The dominant genera *Pediococcus* and *Enterococcus* exhibited significant positive correlations ($|r| > 0.8$, $p < 0.05$) with AN, TAs, TPPs, free isoflavones, and WSE. They were also significantly correlated with aldehydes and amines among the volatile components, a pattern not observed during the koji-making stage. Among the nondominant bacteria, *Staphylococcus* showed positive correlations with methyl linolenate, heptadecanoic acid, and ASE, while *Nitrospira* was correlated with ketones and certain esters. Fungal contributions were less extensive, with four *Aspergillus* species showing significant associations with glycerol content.

Discussions

Indicators reflecting biochemical transformation and product quality evaluationas of SSP

As a functional food, *SSP* requires objective and reliable quality control indicators to ensure product safety, consistency, and efficacy. The current Ch. P. 2020 specifies two main criteria: (1) a minimum total content of 0.04% for daidzein and genistein, and (2) the absence of detectable protein residues via the biuret reaction. However, our findings highlight several limitations in these criteria for assessing fermentation adequacy and product uniformity.

Notably, by the end of the koji-making stage, the total isoflavone content already reaches 0.049% (Figure 3B), satisfying the pharmacopoeial standard even before the onset of post-fermentation. This observation indicates that the current standard fails to adequately reflect the biochemical maturity of *SSP*, which is consistent with previous findings (Wang *et al.*, 2024). In our data, complete hydrolysis of isoflavone glycosides requires at least 12 days of post-fermentation. Because free isoflavones possess higher biological activity than their glycoside counterparts, sufficient fermentation is necessary to ensure full conversion of glycosides into free forms, thereby optimizing the utilization of bioactive resources. Therefore, we propose including at least one isoflavone glycoside (e.g., daidzin or genistin) as a negative marker to better evaluate fermentation completeness and product quality.

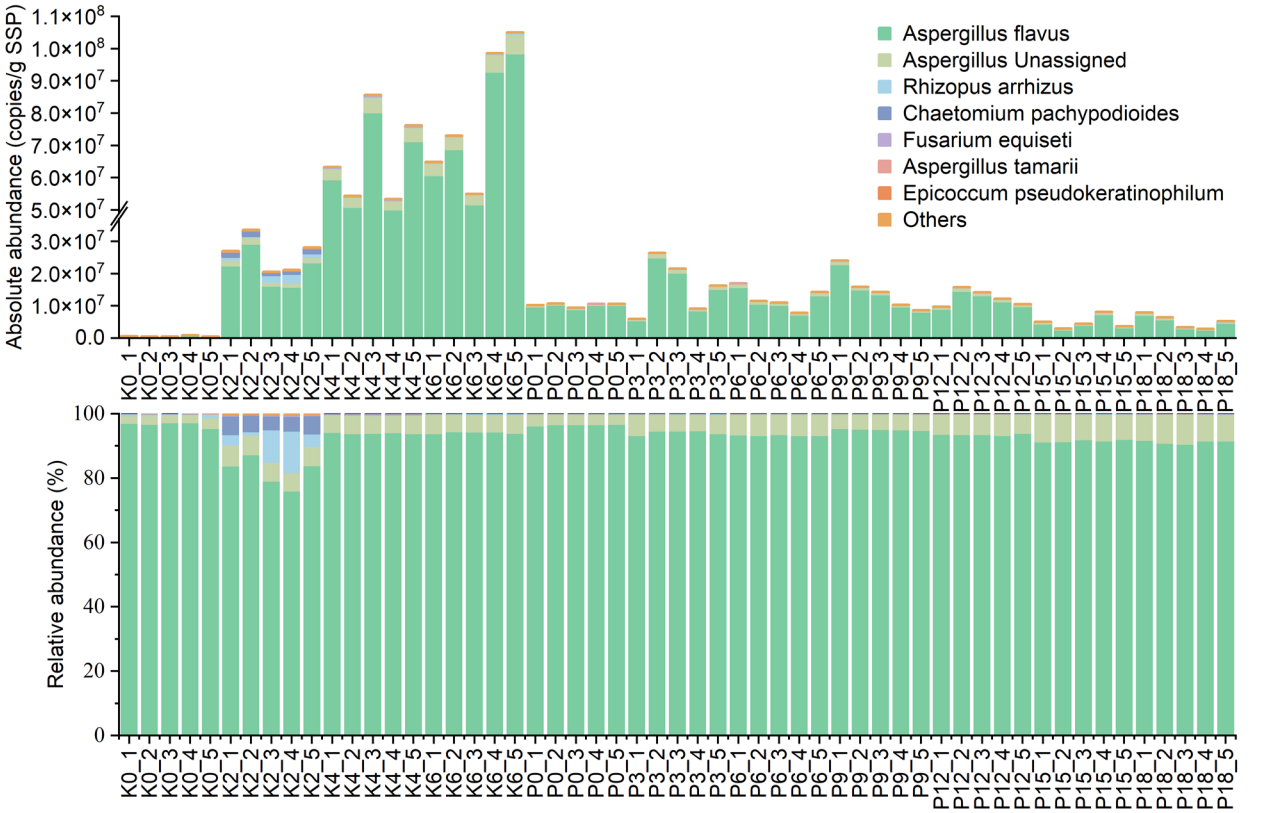

Figure 9. Fungal community composition at the species level during *SSP* fermentation. (A) Absolute abundance. (B) Relative abundance. K0, K2, K4, and K6: samples collected at 0, 2, 4, and 6 days during the koji-making stage; P0, P3, P6, P9, P12, P15, and P18: samples collected at 0, 3, 6, 9, 12, 15, and 18 days during the post-fermentation stage. PS18: steamed product after 18 days of post-fermentation. Data represent mean ± SD, *n* = 5.

In addition, the biuret reaction becomes unreliable after 6 days of post-fermentation, as dark-colored extracts interfere with the colorimetric response (Figure A4). To address this limitation, we identify AN as an alternative indicator that effectively differentiates fermentation stages by reflecting the degree of protein hydrolysis. This concept draws inspiration from quality monitoring systems applied in *Douchi* production, where AN serves as a key marker for proteolytic progress. Interestingly, AN tends to stabilize toward the end of both the koji-making and post-fermentation stages. This plateau likely indicates that microbial protein utilization reaches a steady state, suggesting that nitrogen metabolism slows as the microbial community approaches equilibrium. Similar trends of AN during fermentation have also been reported in other soybean-based fermented foods such as *Douchi*, where AN dynamic reflects the progression of protein hydrolysis (Kumari *et al.*, 2023; Li *et al.*, 2023). Therefore, incorporating AN as a quantitative parameter in industrial production helps determine the optimal fermentation endpoint, reduce batch-to-batch variation, and enhance process consistency. Compared with the color-based biuret assay—which is subjective and easily affected by dark extracts—AN measurement provides an objective, reliable, and quantifiable metric for monitoring protein degradation during fermentation.

Furthermore, we observe that TPPs, WSE, ASE, and TAs increase progressively during fermentation. Although often considered secondary indicators, these parameters effectively reflect the underlying biochemical transformations that determine *SSP* quality. Maintaining an appropriate TAs level helps suppress undesirable microbial growth, which in turn stabilizes the fermentation environment and enhances both safety and reproducibility. Meanwhile, TPP accumulation is generally associated with enhanced antioxidant capacity, as seen in other fermented soybean products where phenolic compounds and free radical–scavenging activities increase over time (He *et al.*, 2024; Kim *et al.*, 2018). WSE and ASE provide complementary insights into fermentation dynamics. WSE, enriched in soluble proteins, peptides, and free amino acids, accumulates with proteolysis and contributes to both flavor complexity and bioactivity. ASE primarily reflects the release and transformation of lipid-soluble and moderately polar compounds, including phenolics and aroma precursors (Ahnan-Winarno *et al.*, 2021). Integrating these indicators into process

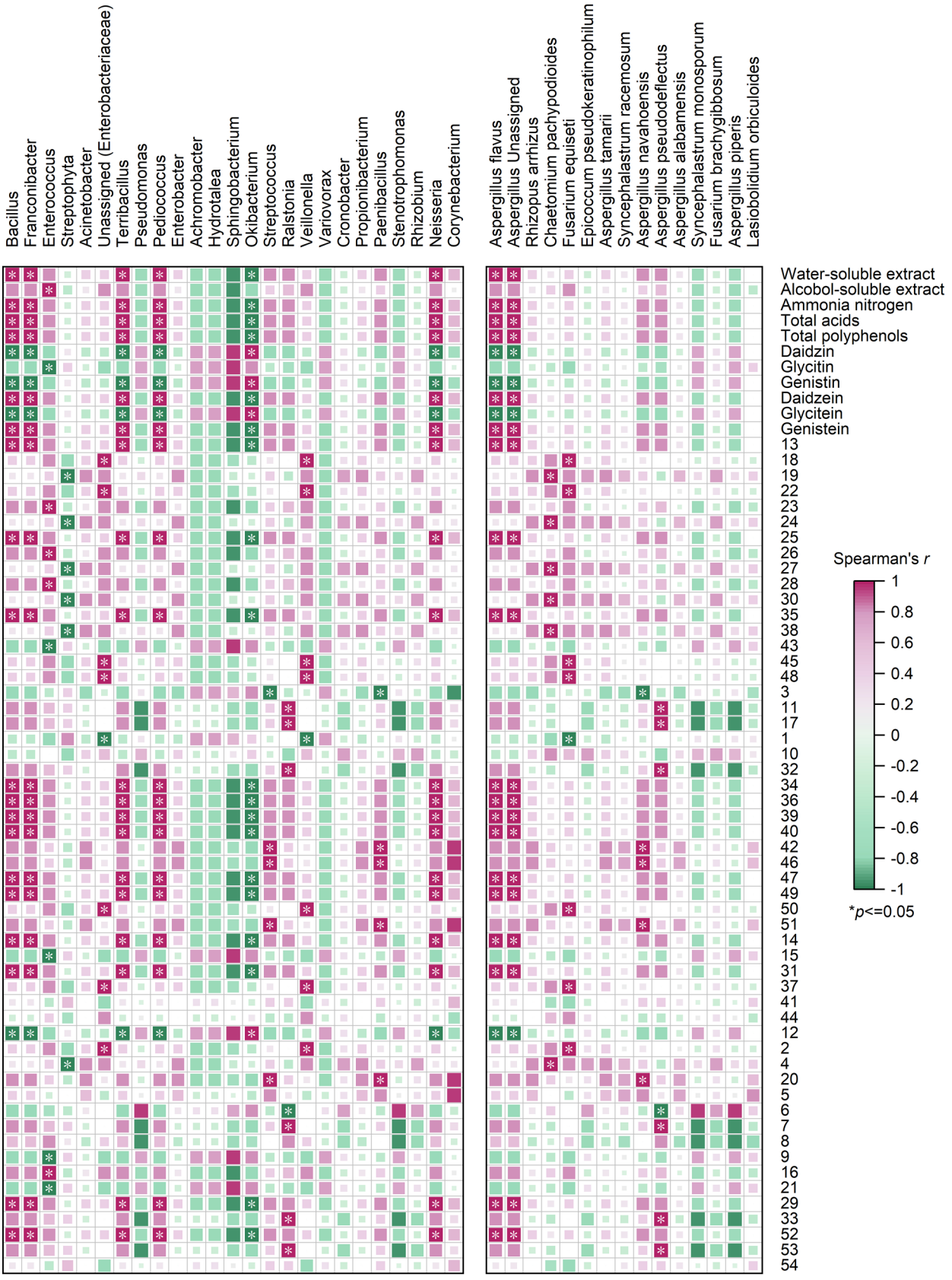

Figure 10. Spearman correlation between *SSP* components and microorganisms during the koji-making stage. Vertical axis: numerical identifiers corresponding to peak assignments in Figure 5. Correlation analysis performed across time points using component data (n = 5) and microorganism data (n = 3). Significant correlations indicated by $|r| > 0.8$, $p < 0.05$.

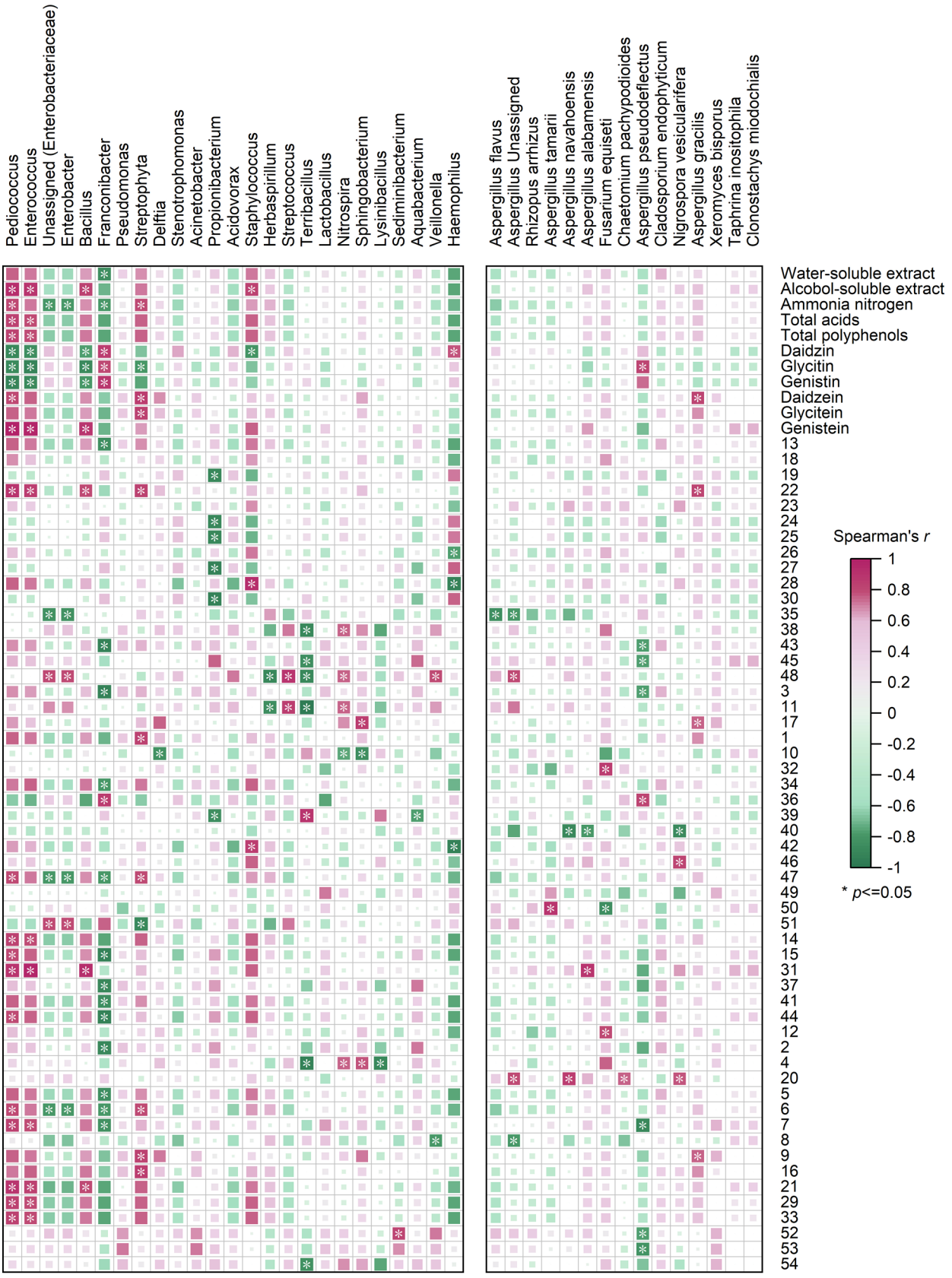

Figure 11. Spearman correlation between *SSP* components and microorganisms during the post-fermentation stage. Vertical axis: numerical identifiers corresponding to peak assignments in Figure 5. Correlation analysis performed across time points using component data (n = 5) and microorganism data (n = 3). Significant correlations indicated by $|r| > 0.8$, $p < 0.05$.

monitoring allows producers to assess fermentation efficiency and product functionality more accurately, laying the foundation for a multiparameter quality evaluation framework in *SSP* production.

Process parameters guiding fermentation control and production optimization

The quality of *SSP* is closely linked to the control of critical fermentation parameters. In this study, moisture content and TSs emerge as particularly influential. Although TSs do not exhibit a clear overall trend during fermentation, practical observations have revealed their critical role during washing yellow cladding. After the initial fermentation, the soybean seed coat becomes thin and fragile, which makes it challenging to remove surface-adhered mycelia and hydrophobic spores. In our practice, we find that leveraging the foaming properties of TSs allows for effective detachment of these residues using minimal water and gentle stirring with smooth wooden tools. This approach not only markedly improves washing efficiency but also reduces water usage, offering an environmentally friendly solution.

Moisture content constitutes another essential parameter. Unlike fermented soybean products intended for pastes, *SSP* requires intact and discrete beans. In our study, during the post-fermentation stage, beans are taken out and spread every 3 days to maintain a water content of around 55% (Figure 3G). The resulting products demonstrate that, although the seed coat becomes thinner and wrinkled, the beans remain intact (Figure 1). This stability largely stems from the balanced moisture level. Maintaining this equilibrium prevents excessive softening or agglomeration, preserves the granular integrity of the final product, and contributes to improved yield. The observed 55% moisture level may serve as a practical reference for industrial *SSP* production.

Volatile metabolites: both beneficial and potentially risky components

Volatile compounds are key determinants of *SSP*'s characteristic flavor. Our analysis reveals a progressive accumulation of total volatile compounds during fermentation, predominantly esters and acids, consistent with previous reports (Li *et al.*, 2021). By applying thresholds of content >10 μg/g and FC >2, we identify compounds with both beneficial and potentially risky implications. Beneficial compounds include lipids such as linoleic acid and oleic acid, which modulate lipid metabolism (Furse *et al.*, 2022), and ethyl linoleate, which is known for cholesterol- and lipid-lowering effects (Iorizzo *et al.*, 2024).

However, we also observe significant accumulation of amine derivatives, including *N*-(2-phenylethyl) formamide, acemide, oleamide, (*R*-(*Z*))-12-hydroxy-9-octadecenamide, and *N*-(2-phenylethyl) acetamide. Notably, the concentrations of the latter two compounds exceed 100 mg/kg during fermentation, which may pose health risks, such as skin or respiratory irritation and organ toxicity (PubChem, 2025). In addition, the biogenic amine phenylethylamine is detected. Biogenic amines are recognized biological hazards, as excessive intake can cause gastrointestinal discomfort, blood pressure fluctuations, and respiratory allergic reactions (Park *et al.*, 2019). Although international regulations stipulate histamine limits for fish products (e.g., US: 50 mg/kg; EU: 100 mg/kg) (Özogul & Özogul, 2019), no analogous standards exist for fermented soybean products. In this study, phenylethylamine reaches a maximum concentration of 9.67 mg/kg. As this represents only one component of the biogenic amine profile, the cumulative risk from total amines is likely underestimated. This concern is further reinforced by reports showing total biogenic amine levels exceeding 100 mg/kg in commercial *Douchi* products (Toro-Funes *et al.*, 2015), indicating that amine accumulation may pose a potential risk in spontaneously fermented *SSP*.

Nevertheless, the characterization of volatile compounds in this study remains incomplete because of limitations of our GC-MS methodology. In comparison, Guo *et al.* (2024) employ SPME-GC-MS with peak area normalization and detect a broader spectrum of alcohols, including 2,3-butanediol and 1-octen-3-ol. Notably, 2,3-butanediol is also detected in our study, confirming partial overlap between the two analyses. To achieve a more comprehensive understanding of *SSP*'s volatile profile, future studies should incorporate advanced complementary analytical techniques.

Dominant microbes in SSP fermentation

Microbial adaptability to fermentation conditions plays a crucial role in shaping microbial dominance. This study shows that *Bacillus* spp. and *Aspergillus flavus* dominate during the aerobic stage, whereas facultative anaerobes such as *Enterococcus* spp. and *Pediococcus* spp. prevail in the oxygen-limited post-fermentation stage. This pattern of microbial succession clearly reflects a close alignment between microbial physiological traits and the specific environmental conditions at each fermentation stage. Our findings challenge previous reports suggesting that *Bacillus* and *A. flavus* maintain dominance throughout the entire fermentation process. For example, Zhu *et al.* (2015) report *Bacillus* as the predominant genus across all stages. However, their culture conditions appear to

favor *Bacillus* growth, potentially masking the actual dominance of anaerobic bacteria during the post-fermentation phase. Similarly, Wang *et al.* (2024) report that *A. flavus* and *Rhizopus* spp. are dominant during the post-fermentation stage. However, given that both fungi are obligate aerobes, it is unlikely that they truly predominate under oxygen-limited conditions. This discrepancy likely results from methodological limitations. When the absolute abundance of these fungi is low, the absence of other fungal taxa may still yield artificially high relative abundance values, leading to a misleading inference that they are dominant species. Therefore, relative quantification alone cannot accurately capture the true microbial abundance across different fermentation stages. This interpretation is further supported by our comparative data (Figure 9), and similar methodological artifacts have been documented in other studies (Bruijning *et al.*, 2023; Tkacz *et al.*, 2018).

During the post-fermentation stage of *SSP*, *Enterococcus* and *Pediococcus* play dominant and functionally significant roles, consistent with observations in the anaerobic fermentation of Korean doenjang (Kim *et al.*, 2018). Both genera are well recognized for their ability to produce diverse bioactive metabolites. For instance, specific strains of *Enterococcus* (e.g., *E. avium* and *E. faecium*) are associated with the synthesis of γ-aminobutyric acid (GABA) (Xiong *et al.*, 2019). Likewise, *Pediococcus pentosaceus* is reported to enhance the accumulation of polyphenols, alcohols, and flavonoids in mulberry leaf (Zhuo *et al.*, 2023). In addition, certain *Pediococcus* strains produce pediocins that inhibit spoilage organisms and pathogens, including *Listeria monocytogenes* (Porto *et al.*, 2017). Our correlational analyses have further demonstrated significant associations between these genera and beneficial metabolites, such as isoflavones and flavor-active acids and esters. The co-occurrence of *Pediococcus* and *Enterococcus*, together with their similar correlation patterns toward key metabolites, suggests a potential functional synergy in shaping the characteristics of fermentation products. Although the underlying mechanism of this cooperation has not yet been elucidated, it represents a promising direction for future research.

Dominant microbes promote both beneficial and potentially risky components

In naturally fermented ecosystems, dominant microbes play indispensable roles in shaping the biochemical profile of the product, yet their metabolic versatility also confers a degree of risk. Consistent with previous findings, *Bacillus*, *Pediococcus*, and *Enterococcus* facilitate the accumulation of bioactive components such as free isoflavones, TPPs, AN, and TAs; however, their proliferation is also associated with the formation of potentially harmful metabolites, including 5-isobutyl-2-isopropyl-3-methoxypyrazine, N-(2-phenylethyl) acetamide, N-(2-phenylethyl) formamide, and N-(2-hydroxyethyl) acetamide (Azizoglu *et al.*, 2023; Lee *et al.*, 2021). In particular, *Pediococcus* and *Enterococcus*, though widely recognized as beneficial fermentation starters, include strains with strong amino acid decarboxylase activity that can convert amino acids into biogenic amines—especially under prolonged or anaerobic fermentation conditions (Barbieri *et al.*, 2019; Montanari *et al.*, 2022). This explains the observed increase in phenylethylamine levels during post-fermentation, which aligns with previous evidence that extended fermentation favors amine accumulation (Jia & Yu, 2022). Therefore, precise control of fermentation duration is critical to prevent excessive amine formation while maintaining the desired product quality. Interestingly, our results reveal that subsequent steaming treatment markedly reduced amine levels while enhancing ester formation, indicating that thermal post-processing serves as an effective strategy to mitigate potential toxic risks while improving flavor characteristics.

Furthermore, several studies have reported that specific strains of *Lactobacillus* and *Bifidobacterium* possess amine-degrading capabilities (Shao *et al.*, 2022), suggesting that microbial modulation offers another feasible approach to enhance product safety. Taken together, these findings underscore the dual attributes of dominant microbial communities in spontaneous fermentation. Future work should focus on the targeted screening and application of low amine-producing or amine-degrading strains to gradually transition traditional spontaneous fermentation toward controlled, starter-guided fermentation systems, thereby enabling more predictable and safer production of *SSP* with improved functional quality.

Moreover, the substantial presence of *Aspergillus flavus* during the koji-making stage warrants particular attention because of its potential to produce aflatoxins (Jallow *et al.*, 2021). In a previous market survey, Qiu et al. (2019) detect total aflatoxin exceeding 10 ng/g in 2 out of 13 samples, surpassing both the Ch. P. 2020 limit (5 ng/g) and the EFSA threshold for cereal products (4 ng/g) (Garcia-Alvarez-Coque *et al.*, 2020). However, Li *et al.* (2020) report aflatoxins levels below 1 ng/g in 22 commercial *SSP* products. In addition, aflatoxin levels accumulate in *SSP* up to P6 but become undetectable by P12 (Ma *et al.*, 2022), suggesting that aflatoxin content is controllable through proper fermentation. Taken together, although *A. flavus* may pose a risk, aflatoxin levels in *SSP* are generally controllable. This control is likely achieved through appropriate fermentation practices, including the physical removal of the yellow cladding and the subsequent degradation by post-fermentation microbes such as *Bacillus* and *Pediococcus* (Ren *et al.*, 2020). To ensure

that aflatoxin levels remain at safe, low concentrations, it is essential to further investigate the effectiveness of the washing process in removing aflatoxins and the role of dominant microbes in post-fermentation in degrading these toxins. By rigorously controlling the washing process, selecting appropriate post-fermentation strains, and optimizing post-fermentation conditions, the risk of toxin accumulation can be minimized.

Conclusion

This study elucidates the dynamic changes of microbial communities during *SSP* fermentation through absolute quantification sequencing. It reveals stage-specific patterns of dominant microbial taxa and their functional associations with key quality components, while also highlighting potential safety risks posed by certain microbes, emphasizing the importance of integrating quality and safety management in *SSP* production. The findings provide a scientific basis for the quantitative development of standardized and safe starter cultures and for improving *SSP* quality. By accounting for fluctuations in total microbial load, absolute quantification sequencing offers a more accurate assessment of microbial community dynamics than conventional methods. This approach is particularly valuable in complex microbial ecosystems, where it can be used to monitor the accumulation of key risk genera, identify core functional microbiota, and optimize microbial consortia. Nevertheless, its taxonomic resolution is currently limited for precise species-level identification and quantification. To address this limitation, long-read genome sequencing can be integrated, or genus-specific identification and quantification methods can be developed for dominant taxa, thereby achieving higher taxonomic resolution, accurate species-level abundance determination, more precise risk assessment, improved process control, and enhanced product quality in fermentation systems.

Data Availability Statement

The sequencing datasets generated for this study have been deposited in NCBI database (BioProject No. PRJNA1184323). All other data supporting the findings of this study are included in the article and its Supplementary Materials. Further inquiries can be directed to the corresponding author.

Author Contributions

Conceptualization, formal analysis, and methodology were done by C.Y.; software was the responsibility of G.H.; validation was looked into by C.Y., M.G., K.F., and C.H.; investigation was done by C.Y. and J.L.; resources was the concern of D.J. and Y.Y.; data curation was the responsibility of C.Y. and J.L.; writing—original draft preparation was done by C.Y.; writing—review and editing was done by C.Y., C.H., and S.M.; visualization was carried out by C.Y. and K.F.; supervision was done by Y.Y.; project administration and funding acquisition were done by Y.Y. All authors have read and agreed to the published version of the manuscript.

Conflicts of Interest

The authors declare no conflict of interest.

Funding

This research was funded by National Natural Science Foundation of China, grant No. 81773840.

References

Ahnan-Winarno, A.D., Cordeiro, L., Winarno, F.G., Gibbons, J. and Xiao, H. 2021. Tempeh: A semicentennial review on its health benefits, fermentation, safety, processing, sustainability, and affordability. Comprehensive Reviews in Food Science and Food Safety 20(2): 1717–1767. https://doi.org/10.1111/1541-4337.12710

An, F., Wu, J., Feng, Y., Pan, G., Ma, Y., Jiang, J., Yang, X., Xue, R., Wu, R. and Zhao, M. 2023. A systematic review on the flavor of soy-based fermented foods: Core fermentation microbiome, multisensory flavor substances, key enzymes, and metabolic pathways. Comprehensive Reviews in Food Science and Food Safety 22(4): 2773–2801. https://doi.org/10.1111/1541-4337.13162

Azizoglu, U., Salehi Jouzani, G., Sansinenea, E. and Sanchis-Borja, V. 2023. Biotechnological advances in Bacillus thuringiensis and its toxins: Recent updates. Reviews in Environmental Science and Bio/Technology 22(2): 319–348. https://doi.org/10.1007/s11157-023-09652-5

Barbieri, F., Montanari, C., Gardini, F. and Tabanelli, G. 2019. Biogenic amine production by lactic acid bacteria: A review. Foods 8(1): 17. https://www.mdpi.com/2304-8158/8/1/17

Bolyen, E., Rideout, J.R., Dillon, M.R., Bokulich, N.A., Abnet, C.C., Al-Ghalith, G.A., Alexander, H., Alm, E.J., Arumugam, M., Asnicar, F., Bai, Y., Bisanz, J.E., Bittinger, K., Brejnrod, A., Brislawn, C.J., Brown, C.T., Callahan, B.J., Caraballo-Rodríguez, A.M., Chase, J., . . . Caporaso, J.G. 2019. Reproducible, interactive, scalable and extensible microbiome data science using QIIME 2. Nature Biotechnology 37(8): 852–857. https://doi.org/10.1038/s41587-019-0209-9

Bruijning, M., Ayroles, J.F., Henry, L.P., Koskella, B., Meyer, K.M. and Metcalf, C.J.E. 2023. Relative abundance data can misrepresent heritability of the microbiome. Microbiome 11(1): 222. https://doi.org/10.1186/s40168-023-01669-w

Callahan, B.J., McMurdie, P.J., Rosen, M.J., Han, A.W., Johnson, A.J. and Holmes, S.P. 2016. DADA2: High-resolution sample inference from Illumina amplicon data. Nature Methods 13(7): 581–583. https://doi.org/10.1038/nmeth.3869

Furse, S., Virtue, S., Snowden, S.G., Vidal-Puig, A., Stevenson, P.C., Chiarugi, D. and Koulman, A. 2022. Dietary PUFAs drive diverse system-level changes in lipid metabolism. Molecular Metabolism 59: 101457. https://doi.org/10.1016/j.molmet.2022.101457

Gao, X., Ohlander, M., Jeppsson, N., Björk, L. and Trajkovski, V. 2000. Changes in antioxidant effects and their relationship to phytonutrients in fruits of sea buckthorn (Hippophae rhamnoides L.) during maturation. Journal of Agricultural and Food Chemistry 48(5): 1485–1490. https://doi.org/10.1021/jf991072g

Garcia-Alvarez-Coque, J.M., Taghouti, I. and Martinez-Gomez, V. 2020. Changes in aflatoxin standards: Implications for EU border controls of nut imports. Applied Economic Perspectives and Policy 42(3): 524–541. https://doi.org/10.1093/aepp/ppy036

Guo, Q., Peng, J., Zhao, J., Yue, J., Huang, Y. and Shao, B. 2024. Correlation between microbial communities and volatile flavor compounds in the fermentation of Semen Sojae Praeparatum. LWT-Food Science and Technology 198: 116009. https://doi.org/10.1016/j.lwt.2024.116009

He, M., Peng, Q., Xu, X., Shi, B. and Qiao, Y. 2024. Antioxidant capacities and non-volatile metabolites changes after solid-state fermentation of soybean using oyster mushroom (Pleurotus ostreatus) mycelium. Frontiers in Nutrition 11: 1509341. https://doi.org/10.3389/fnut.2024.1509341

Iorizzo, M., Di Martino, C., Letizia, F., Crawford, T.W. and Paventi, G. 2024. Production of conjugated linoleic acid (CLA) by Lactiplantibacillus plantarum: A review with emphasis on fermented foods. Foods 13(7): 975. https://doi.org/10.3390/foods13070975

Jallow, A., Xie, H., Tang, X., Qi, Z. and Li, P. 2021. Worldwide aflatoxin contamination of agricultural products and foods: From occurrence to control. Comprehensive Reviews in Food Science and Food Safety 20(3): 2332–2381. https://doi.org/10.1111/1541-4337.12734

Jia, T. and Yu, Z. 2022. Effect of temperature and fermentation time on fermentation characteristics and Biogenic Amine Formation of Oat Silage. Fermentation 8(8): 352. https://doi.org/10.3390/fermentation8080352

Jiang, Z., Fang, O., Xiu, L. and Wang, T. 2019. Detection method of bacterial flora composition and absolute content based on internal reference sequence (Patent No. CN109943654A). State Intellectual Property Office of the P. R. C.

Kim, M.J., Kwak, H.S. and Kim, S.S. 2018. Effects of salinity on bacterial communities, Maillard reactions, isoflavone composition, antioxidation and antiproliferation in Korean fermented soybean paste (doenjang). Food Chemistry 245: 402–409. https://doi.org/10.1016/j.foodchem.2017.10.116

Kumari, R., Sharma, N., Sharma, S., Samurailatpam, S., Padhi, S., Singh, S.P. and Kumar Rai, A. 2023. Production and characterization of bioactive peptides in fermented soybean meal produced using proteolytic Bacillus species isolated from kinema. Food Chemistry 421: 136130. https://doi.org/10.1016/j.foodchem.2023.136130

Lee, J., Nam, S.H., Koo, J.W., Kim, E. and Hwang, T.M. 2021. Comparative evaluation of 2-isopropyl-3-methoxypyrazine, 2-isobutyl-3-methoxypyrazine, and 2,4,6-trichloroanisole degradation by ultraviolet/chlorine and ultraviolet/hydrogen peroxide processes. Chemosphere 279: 130513. https://doi.org/10.1016/j.chemosphere.2021.130513

Li, A., Wang, D., Yang, G., Song, J., Kong, X., Liao, S. and Kan, J. 2023. Effects of post-fermentation temperature on amino nitrogen formation kinetics and physicochemical properties of bacterial-type Douchi from different soybean varieties. Food Science 44(2) : 195–203. https://doi.org/10.7506/spkx1002-6630-20220309-116

Li, G., Long, K., Su, M., Liang, Y., Yang, A. and Xie, X. 2014. Preliminary study on dynamic change of microbial flora in fermentation process to "yellow cladding" of Sojoe semen praeparatum. Chinese Journal of Experimental Traditional Medical Formulae 20(11): 139–142. https://doi.org/10.13422/j.cnki.syfjx.2014110139

Li, N., Lu, Z., Ma, X., Li, M., Guo, X., Cheng, X., Wei, F. and Ma, S. 2020. Definition of key components for quality control on revision of standards of Sojae semen praeparatum. Modern Chinese Medicine 22(7): 1000–1005. https://doi.org/10.13313/j.issn.1673-4890.20200316008

Li, T.N., Zhang, X.R., Zeng, Y.J., Ren, Y.Y., Sun, J.L., Yao, R.C., Wang, Y.J., Wang, J. and Huang, Q.W. 2021. Semen Sojae preparatum as a traditional Chinese medicine: Manufacturing technology, bioactive compounds, microbiology and medicinal function. Food Reviews International 39(2): 896-921. https://doi.org/10.1080/87559129.2021.1928180

Liang, J., Li, D., Shi, R., Wang, J., Guo, S., Ma, Y. and Xiong, K. 2019. Effects of microbial community succession on volatile profiles and biogenic amine during sufu fermentation. LWT-Food Science and Technology 114: 108379. https://doi.org/10.1016/j.lwt.2019.108379

Lim, H.J., Park, I.S., Kim, M.J., Seo, J.W., Ha, G., Yang, H.J., Jeong, D.Y., Kim, S.Y. and Jung, C.H. 2025. Protective effect of Ganjang, a traditional fermented Soy sauce, on colitis-associated colorectal cancer in mice. Foods 14(4): 632. https://doi.org/10.3390/foods14040632

Lin, W.M., Weng, Q.Q., Deng, A.P., Zhao, J.C., Zhang, Y., Zhang, S.L., Yu, B., Zhan, Z.L. and Huang, L.Q. 2021. Literature-based analysis of conversion of components in fermentation process of Sojae semen praeparatum. China Journal of Chinese Materia Medica, 46(9), 2119-2132. https://doi.org/10.19540/j.cnki.cjcmm.20210115.601

Liu, F., Cao, D., Xu, W. and Sui, L. 2022. Dynamic analysis of total flavonoids and polysaccharides in Sojae Semen Praeparatum (SSP) fermentation process. Guiding Journal of Traditional Chinese Medicine and Pharmacy 28(1): 45–48. https://doi.org/10.13862/j.cnki.cn43-1446/r.2022.01.043

Liu, F., Sui, L., Wu, Z., Li, Z., Cao, D. and Xu, W. 2021. Analysis of main microorganisms by ITS technology during fermentation process of Sojae Semen Praeparatum produced in Fujian. Journal of Guizhou University of Traditional Chinese Medicine 43(4): 21–25. https://doi.org/10.16588/j.cnki.issn2096-8426.2021.04.006

Liu, L., Chen, X., Hao, L., Zhang, G., Jin, Z., Li, C., Yang, Y., Rao, J. and Chen, B. 2020. Traditional fermented soybean products: processing, flavor formation, nutritional and biological activities. Critical Reviews in Food Science and Nutrition 62(7): 1971–1989. https://doi.org/10.1080/10408398.2020.1848792

Liu, L., Zhao, J., Lu, D., Zhao, J., Duan, G., Zhu, T. and Hu, Y. 2025. The fermentation law of biogenic amines in the pre-fermentation process is revealed by correlation analysis. Foods 14(4): 583. https://doi.org/10.3390/foods14040583

Ma, S., Li, C., Zhou, H., Li, C., Xie, H., Xie, X., Long, K., Luo, X. and Xie, X. 2022. Analysis of dynamic change law of aflatoxin content in processing of Sojae Semen Praeparatum. Chinese Journal of Hospital Pharmacy 42(21): 2216–2219. https://doi.org/10.13286/j.1001-5213.2022.21.03

Montanari, C., Barbieri, F., Lorenzini, S., Gottardi, D., Šimat, V., Özogul, F., Gardini, F. and Tabanelli, G. 2022. Survival, growth, and biogenic amine production of Enterococcus faecium FC12 in response to extracts and essential oils of Rubus fruticosus and Juniperus oxycedrus. Frontiers in Nutrition 9: 1092172. https://doi.org/10.3389/fnut.2022.1092172

National Pharmacopoeia Commission. 2020. Pharmacopoeia of the People's Republic of China (2020 ed.). China Medical Science Press.

Özogul, Y. and Özogul, F. 2019. Biogenic amines formation, toxicity, regulations in food. In Saad, B. and Tofalo, R. (Eds.), Biogenic amines in food: Analysis, occurrence and toxicity (pp. 1–27). The Royal Society of Chemistry. https://doi.org/10.1039/9781788015813-00001

Park, Y.K., Lee, J.H. and Mah, J.H. 2019. Occurrence and reduction of biogenic amines in traditional Asian fermented soybean foods: A review. Food Chemistry 278: 1–9. https://doi.org/10.1016/j.foodchem.2018.11.045

Porto, M.C.W., Kuniyoshi, T.M., Azevedo, P.O.S., Vitolo, M. and Oliveira, R.P.S. 2017. Pediococcus spp.: An important genus of lactic acid bacteria and pediocin producers. Biotechnology Advances 35(3): 361–374. https://doi.org/10.1016/j.biotechadv.2017.03.004

PubChem. 2025. PubChem compound summary for CID 8249, Phenformin. National Center for Biotechnology Information. Retrieved April 21 2015, from https://pubchem.ncbi.nlm.nih.gov/compound/Phenformin

Qiu, F., Shi, H., Wang, S., Ma, L. and Wang, M. 2019. Safety evaluation of Semen Sojae Preparatum based on simultaneous LC-ESI-MS/MS quantification of aflatoxin B(1), B(2), G(1), G(2) and M(1). Biomedical Chromatography 33(8): e4541. https://doi.org/10.1002/bmc.4541

Ren, X., Zhang, Q., Zhang, W., Mao, J. and Li, P. 2020. Control of aflatoxigenic molds by antagonistic microorganisms: Inhibitory behaviors, bioactive compounds, related mechanisms, and influencing factors. Toxins 12(1): 24. https://doi.org/10.3390/toxins12010024

Shao, X., Xu, B., Chen, C., Li, P. and Luo, H. 2022. The function and mechanism of lactic acid bacteria in the reduction of toxic substances in food: a review. Critical Reviews in Food Science and Nutrition 62(21): 5950–5963. https://doi.org/10.1080/10408398.2021.1895059

Sui, L., Wang, S., Wang, X., Su, L., Xu, H., Xu, W., Chen, L. and Li, H. 2024. Analysis of different strains fermented Douchi by GC×GC-TOFMS and UPLC–Q-TOFMS omics analysis. Foods 13(21): 3521. https://doi.org/10.3390/foods13213521

Tkacz, A., Hortala, M. and Poole, P.S. 2018. Absolute quantitation of microbiota abundance in environmental samples. Microbiome 6(1): 110. https://doi.org/10.1186/s40168-018-0491-7

Toro-Funes, N., Bosch-Fuste, J., Latorre-Moratalla, M.L., Veciana-Nogués, M. T. and Vidal-Carou, M.C. 2015. Biologically active amines in fermented and non-fermented commercial soybean products from the Spanish market. Food Chemistry 173: 1119–1124. https://doi.org/10.1016/j.foodchem.2014.10.118

Wang, B., Shi, Y., Zhang, H., Hu, Y., Chen, H., Liu, Y., Wang, F. and Chen, L. 2024. Influence of microorganisms on flavor substances and functional components of Sojae Semen Praeparatum during fermentation: A study integrating comparative metabolomics and high-throughput sequencing. Food Research International 187: 114405. https://doi.org/10.1016/j.foodres.2024.114405

Wang, P., Wu, Y., Zhang, M. and Gao, X. 2014. Analysis of five active ingredients in 21 Semen Sojae Praeparatum of traditional Chinese medicine from different regions. Chinese Journal of Experimental Traditional Medical Formulae 20(19): 64–67. https://doi.org/10.13422/j.cnki.syfjx.2014190064

Wang, Y., Lin, W., Zhang, S., Yu, B., Nan, T., Kang, L., Li, G., He, X., Zhilai, Z. and Huang, L. 2024. Analysis on quality of Sojae Semen Praeparatum based on traditional quality evaluation. Chinese Journal of Experimental Traditional Medical Formulae 30(1): 31–42. https://doi.org/10.13422/j.cnki.syfjx.20231061

Xiong, J., Ren, J., Zhou, S., Su, M., Wang, L., Weng, M., Xie, W., & Xie, X. 2019. Screening and identification of GABA-producing microbes in fermentation process of Sojae Semen Praeparatum. China Journal of Chinese Materia Medica, 44(11): 2266–2273. https://doi.org/10.19540/j.cnki.cjcmm.20190321.301

Xu, D., Wang, P., Zhang, X., Zhang, J., Sun, Y., Gao, L. and Wang, W. 2020. High-throughput sequencing approach to characterize dynamic changes of the fungal and bacterial communities during the production of sufu, a traditional Chinese fermented soybean food. Food Microbiology 86: 103340. https://doi.org/10.1016/j.fm.2019.103340

Yao, Z., Zhu, Y., Wu, Q. and Xu, Y. 2024. Challenges and perspectives of quantitative microbiome profiling in food fermentations. Critical Reviews in Food Science and Nutrition 64(15): 4995–5015. https://doi.org/10.1080/10408398.2022.2147899

Zhao, C., Wu, S., Zhao, W., Peng, D., Huang, J., Du, B., & Li, P. 2022. Effect of different fermentation methods on the quality and flavor of Semen Sojae Preparatum. Science and Technology of Food Industry 43(23): 144–152. https://doi.org/10.13386/j.issn1002-0306.2022030095

Zhao, C.C., Kim, D.W., & Eun, J.B. 2019. Physicochemical properties and bacterial community dynamics of hongeo, a Korean traditional fermented skate product, during fermentation at 10°C. LWT–Food Science and Technology 104: 109–119. https://doi.org/10.1016/j.lwt.2019.01.048

Zhao, H., Chen, H., Wu, G., Xu, J., Zhu, W., Chen, J., Luo, D. and Guo, S. 2025. Integrative metabolomics—GC-IMS approach to assess metabolic and flavour substance shifts during

fermentation of Yangjiang douchi. Food Chemistry 466: 142199. https://doi.org/10.1016/j.foodchem.2024.142199

Zhu, H., Long, K., Liang, Y., Su, M. and Xie, X. 2015. Dynamic change monitoring of microbe species in fermentation process of Sojoe Semen Praeparatum by Biolog Microbial Identification System. Chinese Journal of Experimental Traditional Medical Formulae 21(17): 14–17. https://doi.org/10.13422/j.cnki.syfjx.2015170014

Zhuo, J., Xuan, J., Chen, Y., Tu, J., Mu, H., Wang, J. and Liu, G. 2023. Increase of γ-aminobutyric acid content and improvement of physicochemical characteristics of mulberry leaf powder by fermentation with a selected lactic acid bacteria strain. LWT–Food Science and Technology 187: 115250. https://doi.org/10.1016/j.lwt.2023.115250

Supplementary

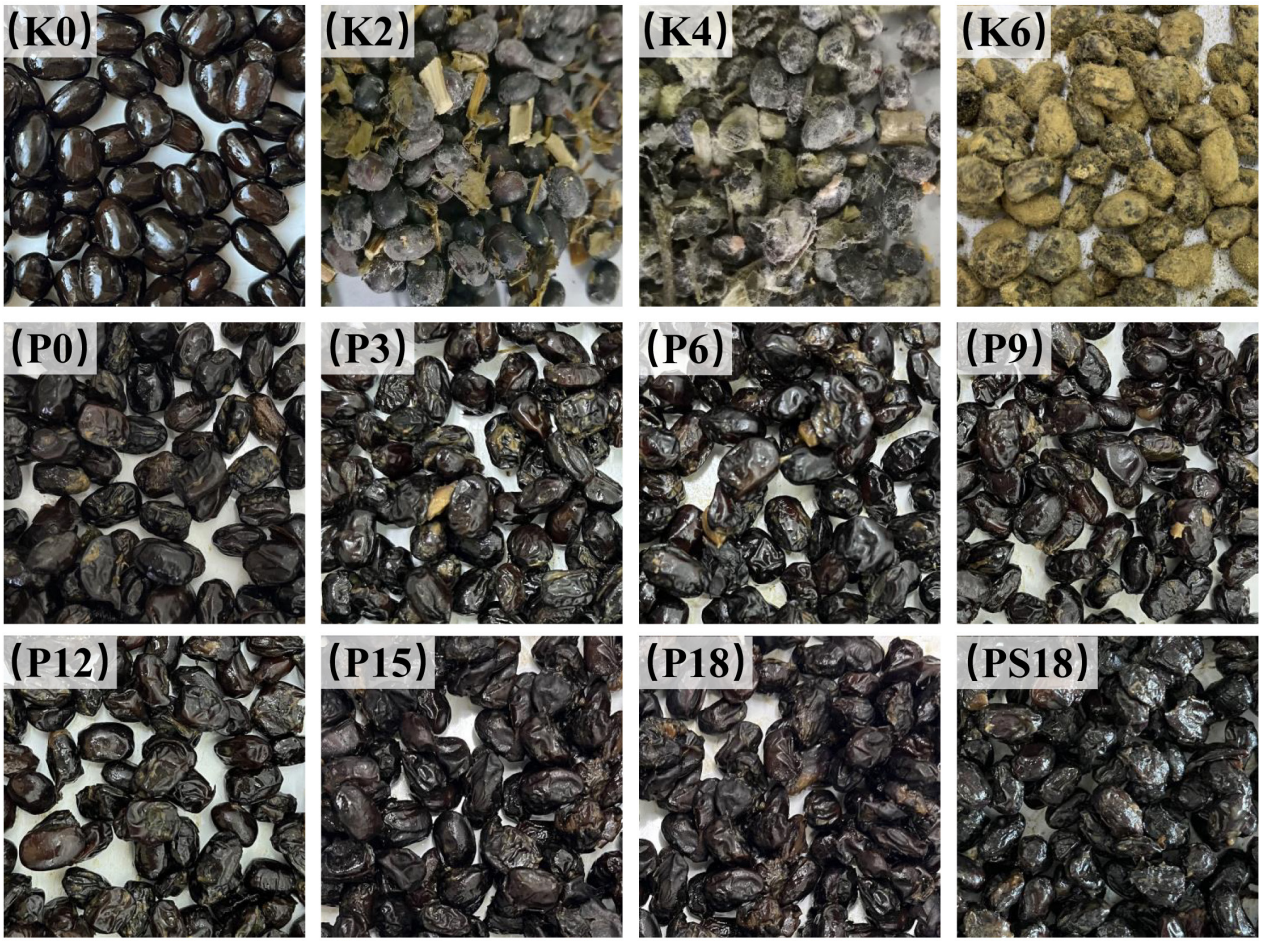

Figure S1. ***Sojae Semen Praeparatum*** **samples at different time points (fresh).**

Figure S2. ***Sojae Semen Praeparatum*** **samples at different time points (dried).**

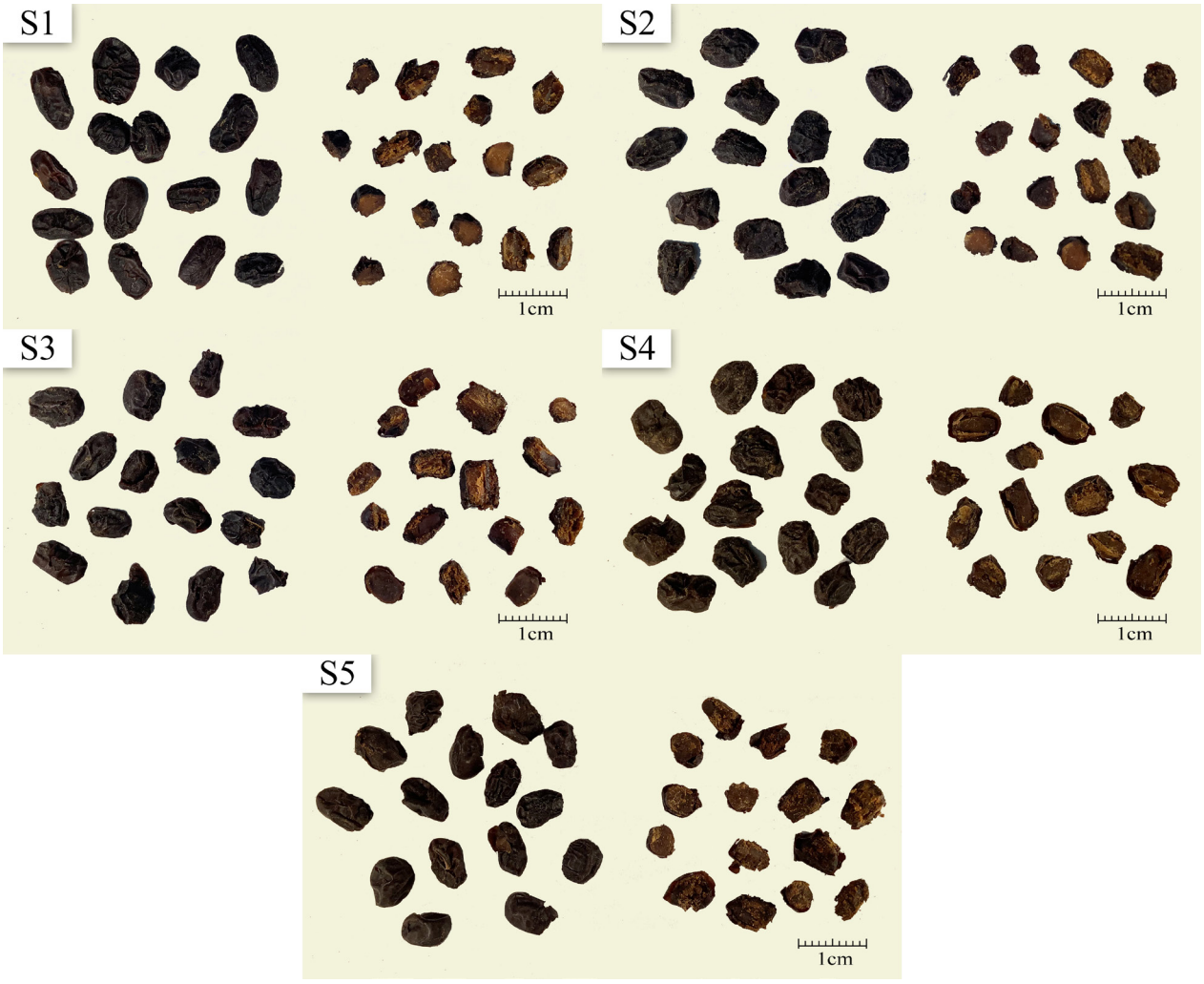

Figure S3. The appearance surface and cross-section view of the five batches of self-made *Sojae Semen Praeparatum*.

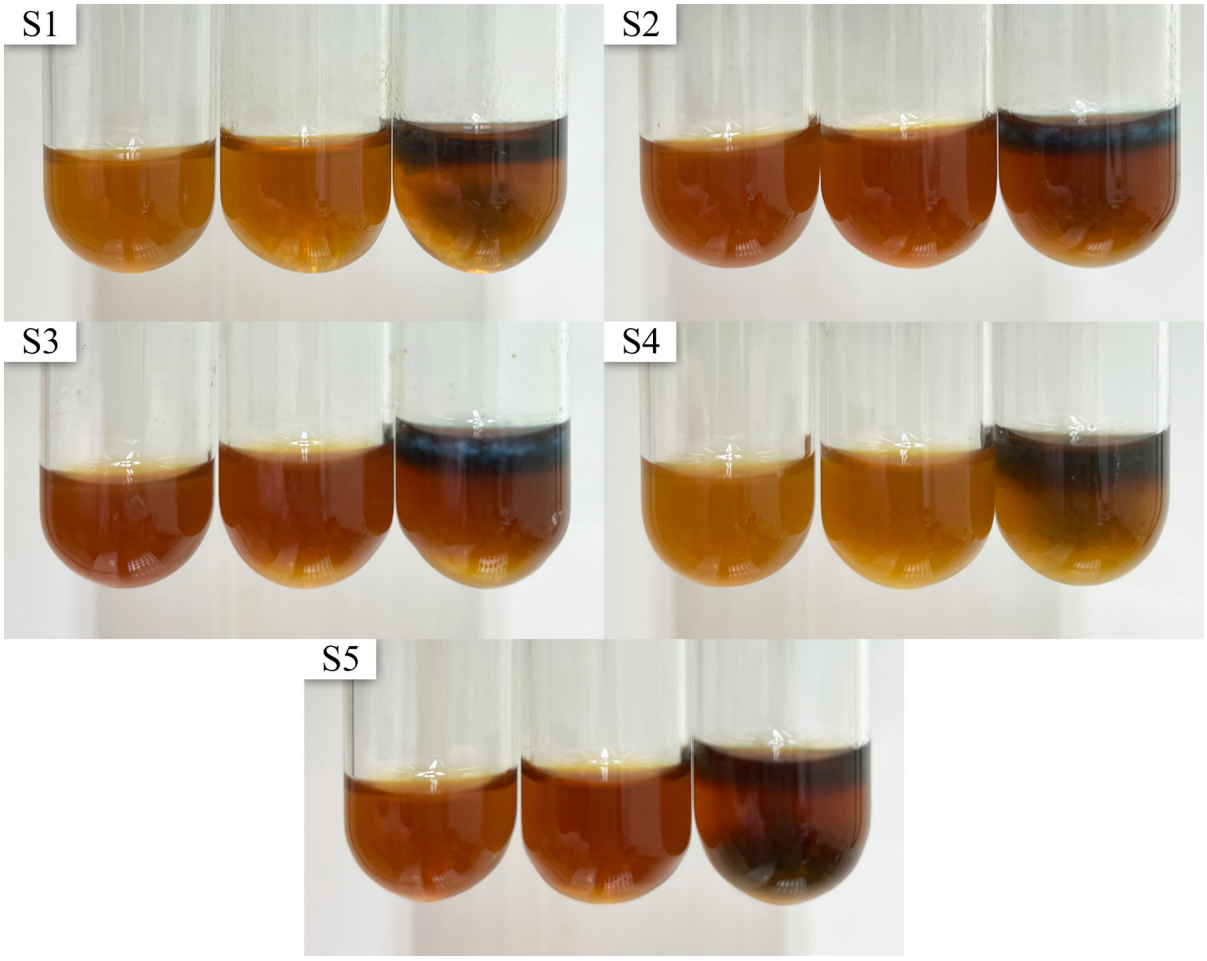

Figure S4. **Purity test (biuret color reaction) of the five batches of self-made *SSP*.**

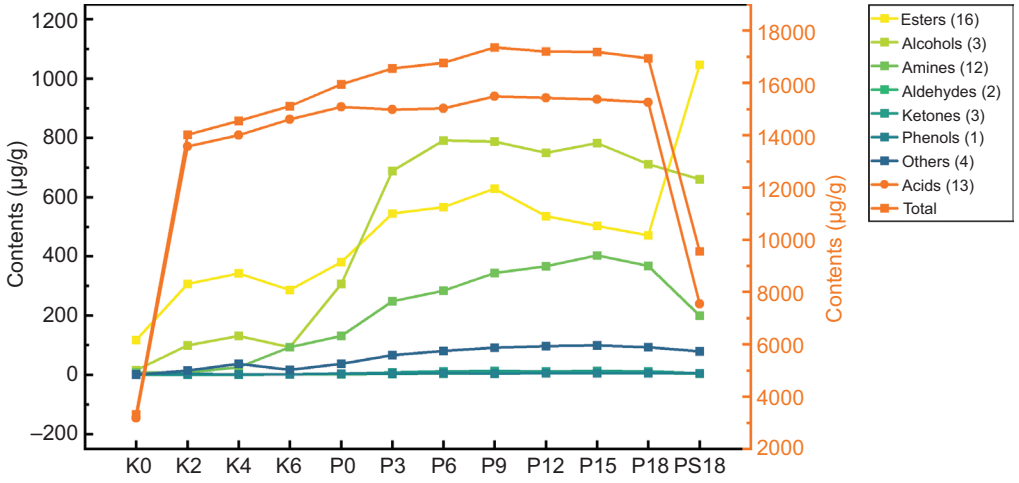

Figure S5. **The types of volatile components and their content changes during the fermentation process of *SSP*.**

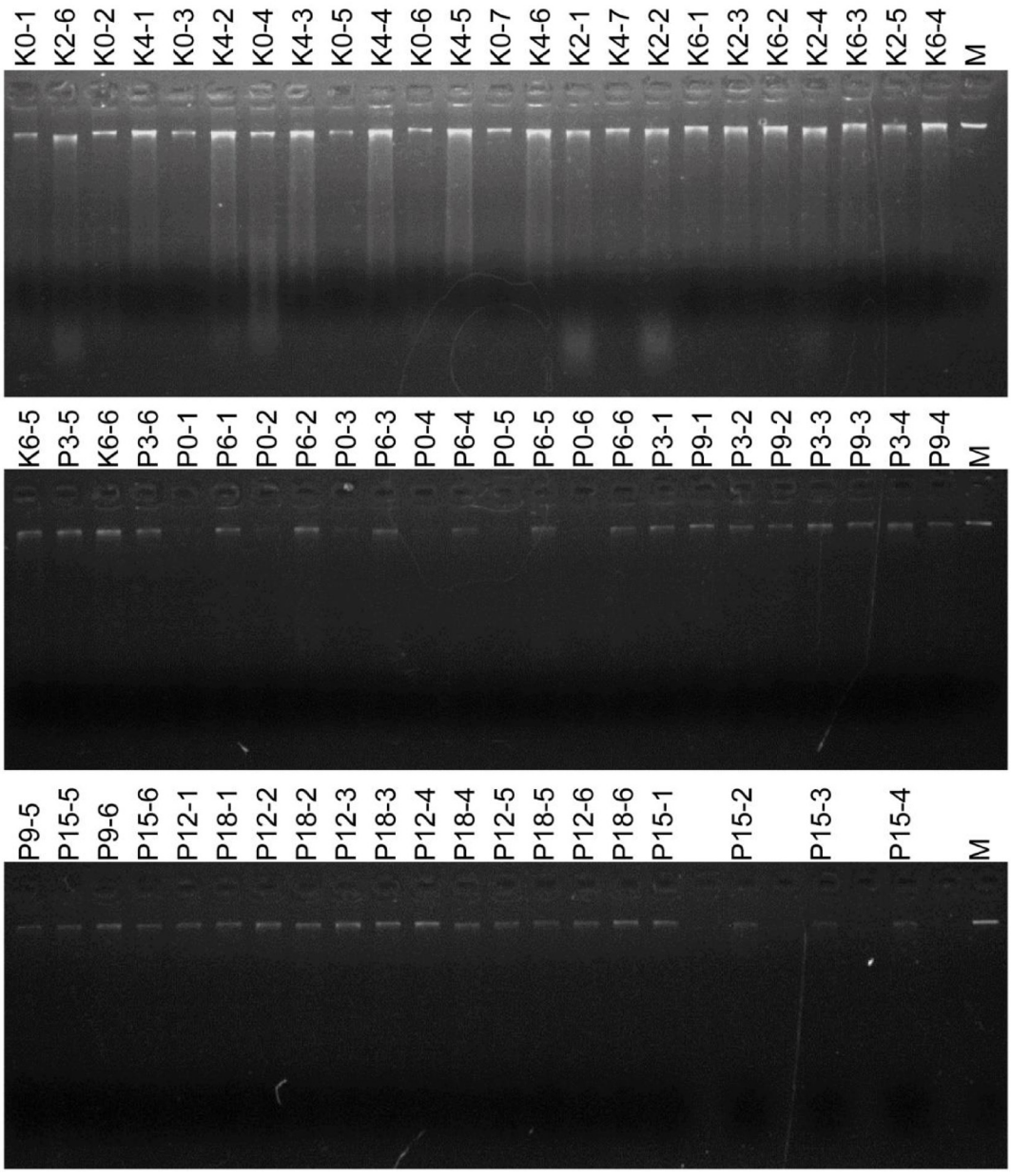

Figure S6. Gel electrophoresis results of microbial genomic DNA of *SSP* samples.

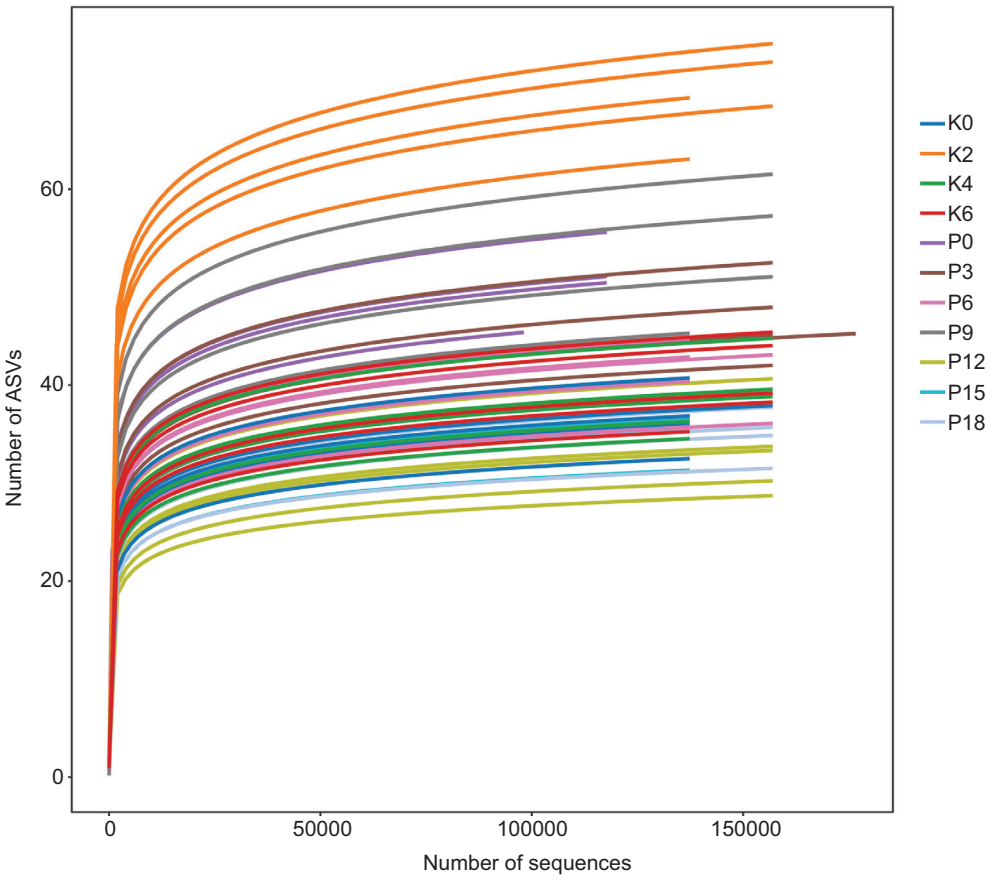

Figure S7. Each curve represents a sample collected at different time points during *SSP* fermentation.

Method Validation of UPLC for the Quantitative Analysis of Isoflavones in *Sojae Semen Praeparatum* (*SSP*)

Specificity

In the test solution prepared from *SSP*, the six analytes—daidzin, glycitin, genistin, daidzein, glycitein, and genistein—were separated from other components. The chromatographic peaks exhibited theoretical plate numbers exceeding 10,000 for each compound.

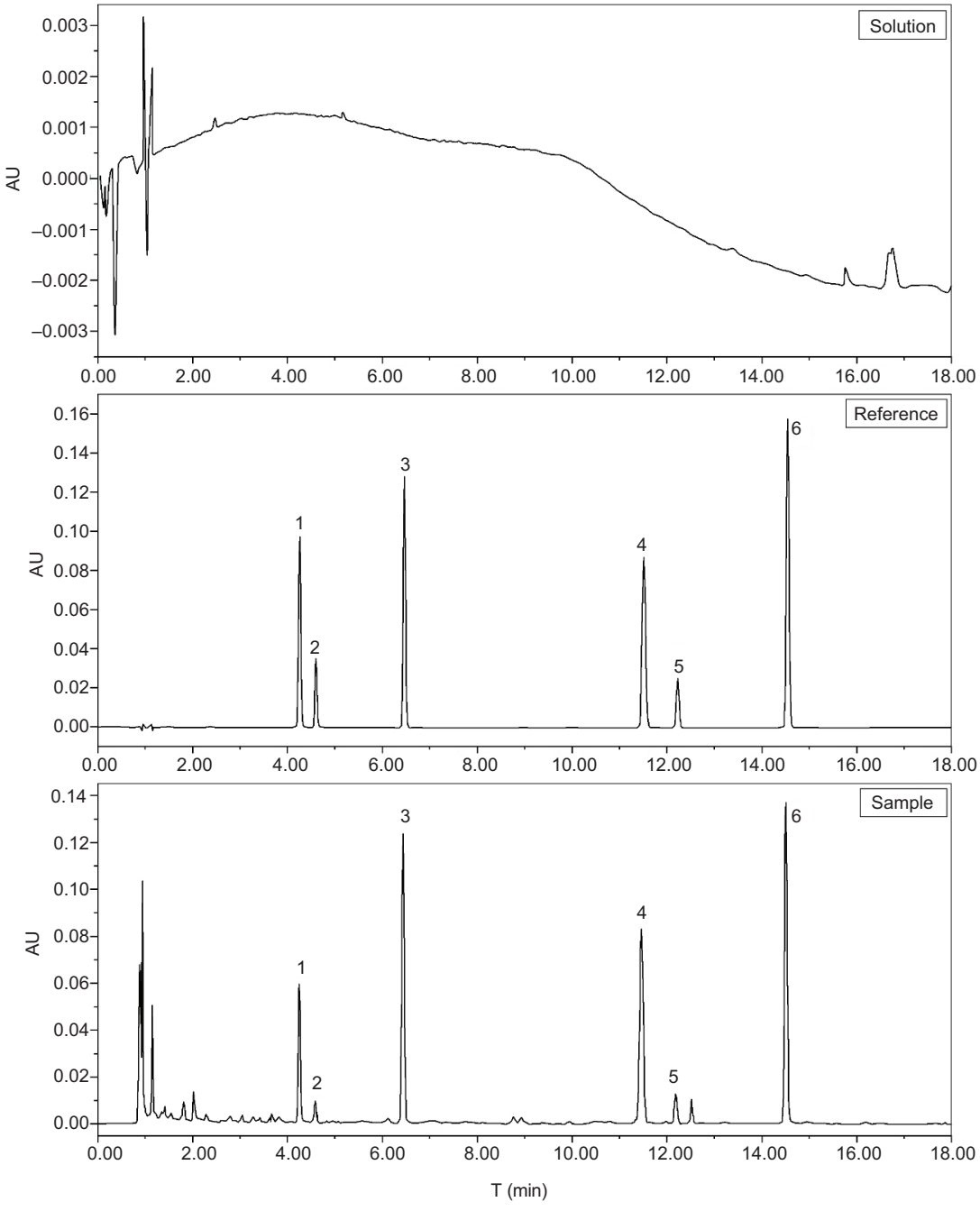

Figure S8. UPLC chromatogram of *Semen Sojae Preparatum* sample solution.

Linear Range

Table S1. Linear range of six isoflavones.

Compound	Regression equation	linear range (μg/mL)	r
Daidzin	Y=15143X-2931.4	0.89–114.30	0.9999
Glycitin	Y=14660X-504.27	0.79–100.70	0.9999
Genistin	Y=20970X-806.55	0.24–103.30	0.9999
Daidzein	Y=22550X-6429.7	0.81–103.80	0.9999
Glycitein	Y=21726X-3046	0.76–48.45	0.9999
Genistein	Y=32003X+2332.6	0.79–101.50	0.9999

Note: X represents the concentration of the analyte in the test solution (μg/mL), and Y denotes the corresponding chromatographic peak area.

Accuracy (spiked recovery)

Spiked recovery was determined by adding the standard to sample at 100% of the nominal concentration in six replicates.

Table S2. Spiked recovery of six isoflavones.

Compound	Sample weight (g)	Original amount (μg)	Spiked amount (μg)	Observed amount (μg)	Recovery (%)	Average recovery (%)	RSD (%)
Daidzin	0.5001	**49.94**	**68.580**	**118.48**	99.94	**102.32**	**1.90**
	0.5002	**49.95**	**68.580**	**120.71**	103.17		
	0.4997	**49.90**	**68.580**	**121.03**	103.71		
	0.4999	**49.92**	**68.580**	**118.03**	99.32		
	0.5002	**49.95**	**68.580**	**120.86**	103.40		
	0.5000	**49.93**	**68.580**	**121.51**	104.37		
Glycitin	0.5001	**26.43**	**32.224**	**58.02**	98.03	**100.15**	**2.52**
	0.5002	**26.43**	**32.224**	**58.65**	99.98		
	0.4997	**26.41**	**32.224**	**59.57**	102.91		
	0.4999	**26.42**	**32.224**	**57.31**	95.88		
	0.5002	**26.43**	**32.224**	**59.14**	101.49		
	0.5000	**26.42**	**32.224**	**59.47**	102.57		
Genistin	0.5001	**10.33**	**41.640**	**52.66**	101.66	**103.51**	**1.23**
	0.5002	**10.33**	**41.640**	**53.51**	103.69		
	0.4997	**10.32**	**41.640**	**54.18**	105.32		
	0.4999	**10.32**	**41.640**	**53.22**	103.02		
	0.5002	**10.33**	**41.640**	**54.00**	104.86		
	0.5000	**10.33**	**41.640**	**53.01**	102.51		
Daidzein	0.5001	**162.94**	**195.144**	**354.62**	98.22	**97.19**	**1.69**
	0.5002	**162.98**	**195.144**	**354.70**	98.25		
	0.4997	**162.81**	**195.144**	**347.47**	94.63		
	0.4999	**162.88**	**195.144**	**351.54**	96.68		
	0.5002	**162.98**	**195.144**	**350.03**	95.85		
	0.5000	**162.91**	**195.144**	**357.07**	99.50		

(*continues*)

Table S2. Continued.

Compound	Sample weight (g)	Original amount (μg)	Spiked amount (μg)	Observed amount (μg)	Recovery (%)	Average recovery (%)	RSD (%)
Glycitein	0.5001	**17.56**	**19.380**	**36.05**	95.41	**97.60**	**2.76**
	0.5002	**17.56**	**19.380**	**37.18**	101.25		
	0.4997	**17.54**	**19.380**	**37.20**	101.42		
	0.4999	**17.55**	**19.380**	**36.28**	96.64		
	0.5002	**17.56**	**19.380**	**35.94**	94.83		
	0.5000	**17.56**	**19.380**	**36.17**	96.06		
Genistein	0.5001	**136.72**	**162.400**	**302.54**	102.11	**101.60**	**2.97**
	0.5002	**136.75**	**162.400**	**305.41**	103.86		
	0.4997	**136.61**	**162.400**	**306.56**	104.65		
	0.4999	**136.67**	**162.400**	**296.17**	98.22		
	0.5002	**136.75**	**162.400**	**293.96**	96.80		
	0.5000	**136.69**	**162.400**	**305.54**	103.97		

Precision

The same test solution was injected six consecutive times. The relative standard deviations (RSD, %) for the peak areas of daidzin, glycitin, genistin, daidzein, glycitein, and genistein were calculated as 0.74%, 0.59%, 0.97%, 0.20%, 1.92%, and 0.09%, respectively, indicating excellent instrument precision.

Repeatability

Six test solution replicates were prepared in parallel. RSD, % for the peak areas of Daidzin, Glycitin, Genistin, Daidzein, Glycitein, and Genistein were calculated as 0.87%, 1.95%, 0.64%, 0.56%, 2.84%, and 0.78%, respectively.

Solution stability

Samples were injected and analyzed at 0 h, 2 h, 4 h, 6 h, 8 h, 12 h, 16 h, 20 h, and 24 h after preparation of the test solution. Each sample was assayed in triplicate at each time point. The RSD, % for the peak areas of daidzin, glycitin, genistin, daidzein, glycitein, and genistein were 0.35%, 2.79%, 2.93%, 0.44%, 0.81%, and 0.47%, respectively. These results demonstrate that the test solution remained stable throughout the 24-h period.